

12

ADA111647



TECHNICAL REPORT RE-81-19

ACTIVE RF SEEKER ANALYSIS FOR LAND COMBAT SEEKERS

R. F. Russell and R. H. Garlough
Advanced Sensors Directorate
US Army Missile Laboratory

April 1981

DTIC
ELECTE
MAR 4 1982
B



U.S. ARMY MISSILE COMMAND

Redstone Arsenal, Alabama 35809

DTIC FILE COPY

Approved for public release; distribution unlimited.

corrected by

DISPOSITION INSTRUCTIONS

DESTROY THIS REPORT WHEN IT IS NO LONGER NEEDED. DO NOT RETURN IT TO THE ORIGINATOR.

DISCLAIMER

THE FINDINGS IN THIS REPORT ARE NOT TO BE CONSTRUED AS AN OFFICIAL DEPARTMENT OF THE ARMY POSITION UNLESS SO DESIGNATED BY OTHER AUTHORIZED DOCUMENTS.

TRADE NAMES

USE OF TRADE NAMES OR MANUFACTURERS IN THIS REPORT DOES NOT CONSTITUTE AN OFFICIAL INDORSEMENT OR APPROVAL OF THE USE OF SUCH COMMERCIAL HARDWARE OR SOFTWARE.

Unclassified

SECURITY CLASSIFICATION OF THIS PAGE (When Data Entered)

REPORT DOCUMENTATION PAGE		READ INSTRUCTIONS BEFORE COMPLETING FORM
1. REPORT NUMBER TR-RE-81-19	2. GOVT ACCESSION NO. AD-A111 647	3. RECIPIENT'S CATALOG NUMBER
4. TITLE (and Subtitle) Active RF Seeker Analysis for Land Combat Seekers		5. TYPE OF REPORT & PERIOD COVERED
		6. PERFORMING ORG. REPORT NUMBER SRI AD-E950 175
7. AUTHOR(s) R.F. Russell and R.H. Garlough		8. CONTRACT OR GRANT NUMBER(s)
9. PERFORMING ORGANIZATION NAME AND ADDRESS Commander, US Army Missile Command ATTN: DRSMI-RE Redstone Arsenal, AL 35878		10. PROGRAM ELEMENT, PROJECT, TASK AREA & WORK UNIT NUMBERS
11. CONTROLLING OFFICE NAME AND ADDRESS Commander, US Army Missile Command ATTN: DRSMI-RE Redstone Arsenal, AL 35878		12. REPORT DATE April 1981
		13. NUMBER OF PAGES 51
14. MONITORING AGENCY NAME & ADDRESS (if different from Controlling Office)		15. SECURITY CLASS. (of this report) Unclassified
		15a. DECLASSIFICATION/DOWNGRADING SCHEDULE
16. DISTRIBUTION STATEMENT (of this Report) Approved for public release; distribution unlimited		
17. DISTRIBUTION STATEMENT (of the abstract entered in Block 20, if different from Report)		
18. SUPPLEMENTARY NOTES		
19. KEY WORDS (Continue on reverse side if necessary and identify by block number) All-weather guidance system RF Seeker Squint Polarization Frequency Discrimination		
20. ABSTRACT (Continue on reverse side if necessary and identify by block number) This report discusses some analysis techniques which apply to all-weather/day-night missile guidance systems against tank type targets using an RF seeker. Those techniques are examined that may be applied to obtain the proper s/c ratio and terminal accuracy, including squint, polarization and frequency discrimination.		

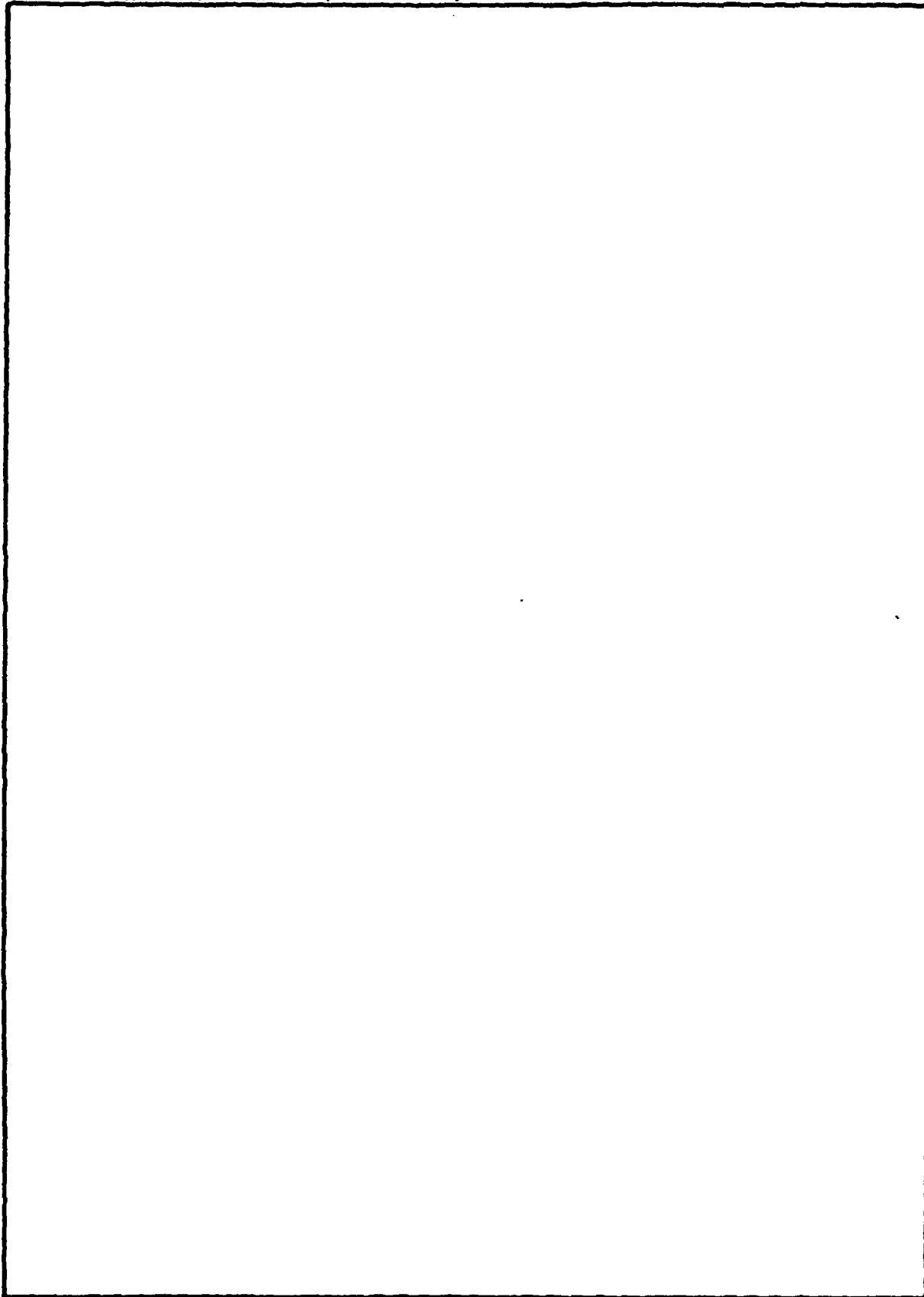
DD FORM 1 JAN 73 1473

EDITION OF 1 NOV 65 IS OBSOLETE

Unclassified

SECURITY CLASSIFICATION OF THIS PAGE (When Data Entered)

SECURITY CLASSIFICATION OF THIS PAGE(When Data Entered)



SECURITY CLASSIFICATION OF THIS PAGE(When Data Entered)

CONTENTS

	PAGE NO.
I. INTRODUCTION	3
II. SEEKER OPERATIONAL ENVIRONMENT	3
III. PARAMETER TRADE-OFFS	3
IV. SIGNAL PROCESSING TECHNIQUES	13
V. ELECTRONIC COUNTERMEASURES (ECM)	24
VI. RADAR ERRORS	26

Accession For	
NTIS GRA&I	<input checked="" type="checkbox"/>
DTIC TAB	<input type="checkbox"/>
Unannounced	<input type="checkbox"/>
Justification	
From	
Distribution/	
Availability Codes	
Avail and/or	
Dist	Special
A	



LIST OF ILLUSTRATIONS

Figure No.		Page No.
1.	Transmitter power required	5
2.	Transmitter power required with atmospheric attenuation ...	7
3.	Transmitter power required with 4 mm of rain.....	8
4.	Clutter area.....	9
5.	Signal-to-clutter ratio as a function of frequency.....	11
6.	Signal to clutter ratio as a function of altitude.....	12
7.	Reflectivity of a 4 mm/hr rain as a function of frequency..	14
8.	Signal-to-clutter as a function of frequency.....	15
9.	Simple CW radar	16
10.	Basic missile borne radar with SAR.....	16
11.	Doppler shift at angles off boresight.....	18
12.	Doppler shift at angles off boresight for different missile velocities.....	19
13.	Signal-to-clutter improvement factor for a 16.5 GHz missile seeker.....	20
14.	Single pulse signal-to-jammer ratio as a function of range - no propagation loss.....	27
15.	Radar pulse shape.....	28
16.	Leading and trailing edge tracker.....	29
17.	Frequency-modulated pulse-compression wave forms.....	30
18.	Compressed pulse with noise.....	32
19.	Range multipath errors.....	34
20.	Typical antenna pattern for multipath (elevation).....	36
21.	Radar errors due to multipath.....	38

I. INTRODUCTION

The primary objective of this technical report is to discuss some analysis techniques which apply to all-weather/day-night missile guidance systems against tank type targets, using an RF type seeker.

The major limitation of an RF seeker system has been the inability to achieve the required signal-to-clutter (S/C) ratio ($\geq 13\text{dB}$) because of very large ground clutter areas intercepted by the antenna beam when using a seeker antenna which has practical aperture dimensions. The problem is magnified when operating against a stationary target, such as an enemy tank stopped to shoot, because the target and clutter doppler are the same.

This report will examine those techniques that may be applied to obtain the proper S/C ratio and terminal accuracy, including squint, polarization, and frequency discrimination.

II. SEEKER OPERATIONAL ENVIRONMENT

An operational environment is specified so that an example design can be postulated. The following example design assumes an all-weather operation requirement consisting of a 30-meter visibility fog (2.3 gm/m^3) or a moderate rain (4 mm/hr). The target has an assumed radar cross section of 100 square meters and a range of 5 kilometers. The missile which houses the RF seeker has a diameter of 15.24 cm.

III. PARAMETER TRADE-OFFS

The preliminary analysis which follows shows the effects on the seeker of aperture size, frequency, and other variables.

a. Transmitted Power

The basic radar equation in its most common form is

$$S/N = P_t G_t A_r \frac{\sigma}{(4\pi)^2 R^4} KTB N_f L_s$$

where S/N = signal-to-noise ratio

K = Boltzmann constant $1.38 \times 10^{-23} \text{ w-sec/}^\circ\text{K}$

B = noise bandwidth of receiver, Hz

T = ambient temperature at the receiver, $^\circ\text{K}$

N_f = receiver noise figure

R = range to target, meters

P_t = transmitter, watts

- G_t = transmitter antenna gain
- A_R = receiver antenna effective area, m^2
- σ = radar cross section, m^2
- L_s = system losses

Antenna gain is related to antenna effective area by the following (assuming common transmitter and receiver antenna):

$$G_t = \frac{4\pi A_r}{\lambda^2}$$

and wavelength is related to frequency by

$$\lambda = c/f$$

where c = speed of light 3×10^8 m/sec

f = carrier frequency

therefore, the basic radar equation becomes

$$P_t = \frac{c^2 (S/N) L_s 4\pi R^4 K T N_f B}{f^2 A_r^2 \sigma}$$

If it is assumed that of a 15.24 cm missile diameter, only 13.97 cm can be utilized in antenna diameter with an aperture efficiency of 55 percent, then A_R becomes

$$A_R = \rho \pi (0.1397/2)^2 = 0.00843 M^2$$

The parameters used for calculating the plot of Figure 1 are shown below. Although these parameters are assumed constant while calculating power required, some of the parameters may vary as a function of frequency in the real world. However, due to differences, system-to-system, math modeling is not practical for the general case. Parameters which will vary, especially above 20 GHz, are antenna efficiency, receiver noise, and system losses.

Assume that the targets of interest have a maximum length of 7.5 meters, then the range resolution should equal the maximum target length. Utilizing a matched receiver, the bandwidth is equal to one over the pulsewidth.

$$\Delta R = c \frac{\tau}{2}$$

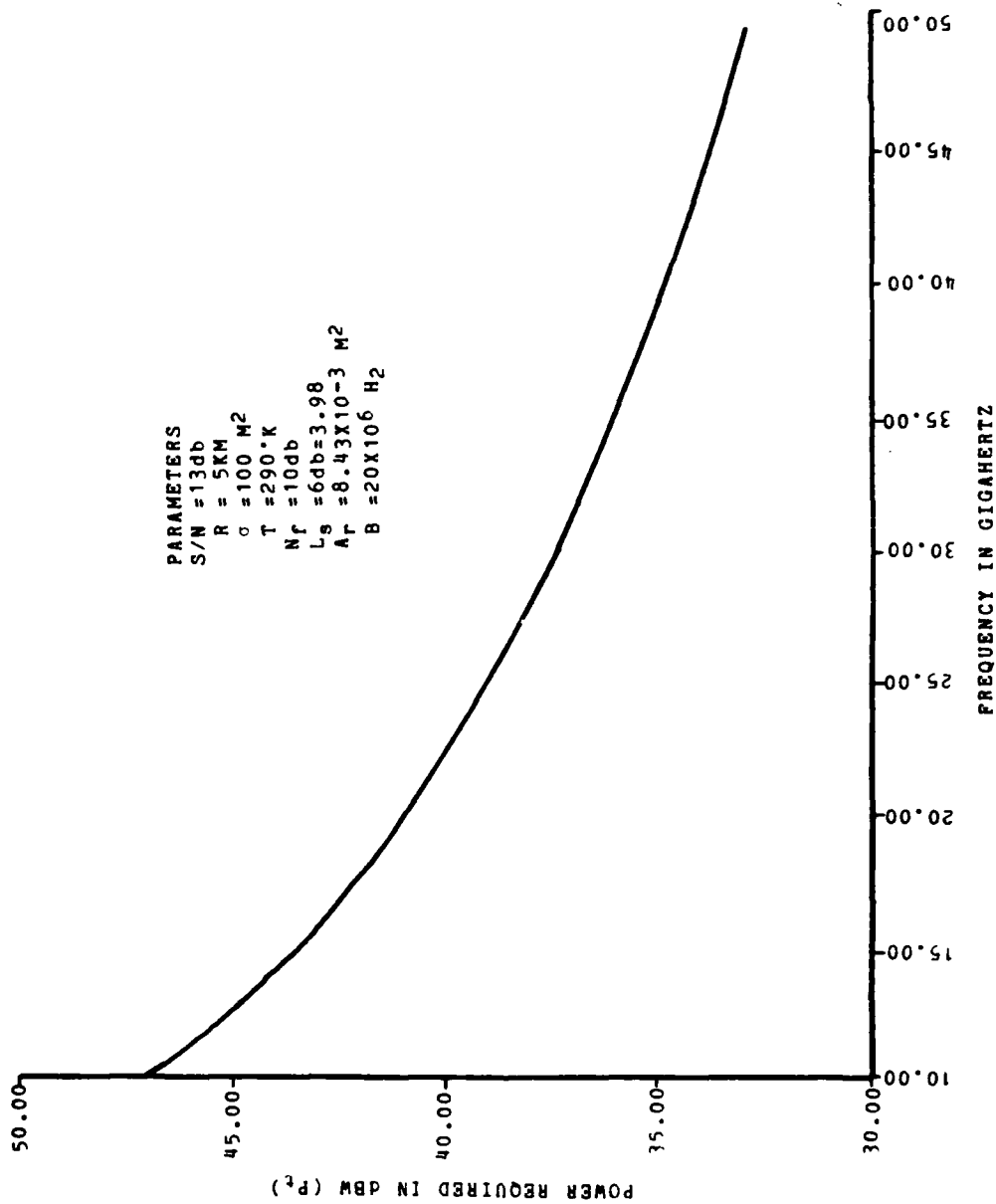


Figure 1. Transmitter power required.

where ΔR is range resolution in meters

τ is pulse width in seconds

therefore,

$$B = \frac{1}{\tau} = 20 \times 10^6 \text{ Hz}$$

where B is bandwidth in Hertz.

Further assumptions required are for the noise figure (N_F) of the receiver and the system losses (L_S)

$$N_F = 10 \text{ dB}$$

$$L_S = 6 \text{ dB}$$

Figure 1 shows the power required on the target as a function of frequency for maintaining 13 dB S/N ratio at 5km range in a clear environment; that is no rain, no fog, and no atmospheric attenuation.

The data presented in Figure 2 shows the power required under the same conditions as Figure 1 with the inclusion of atmospheric attenuation.

Figure 3 shows the power required with 4mm/hr of rain. The rain model is from Radar System Analysis, by D.K. Barton, Prentice-Hall, 1965, page 472. Figure 3 includes the effects of attenuation only and does not include the clutter return due to rain. Rain clutter is discussed in Section c.

b. Signal-to-Clutter Ratio

Assuming that some form of range discrimination or gating is used, the signal-to-clutter ratio is the ratio of the desired target (σT) to clutter ($\sigma^o A_p$) where σ^o is the normalized cross section in square meters per square meter, and A_p is the projected area of the beam on the clutter area as shown in Figure 4.

Therefore, the projected clutter area (A_p) is the range-to-target distance multiplied by the antenna beamwidth multiplied by the range cell depth (ΔR).

$$A_p \approx R (\theta_B) \Delta R$$

when θ_B is in radians

This projected area is a function of frequency because the beamwidth is a function of frequency. Therefore, A_p becomes

$$A_p = \left(\frac{\Delta R}{\cos \beta} \right) \left(\frac{3.66 \times 10^8}{Df} \right) R$$

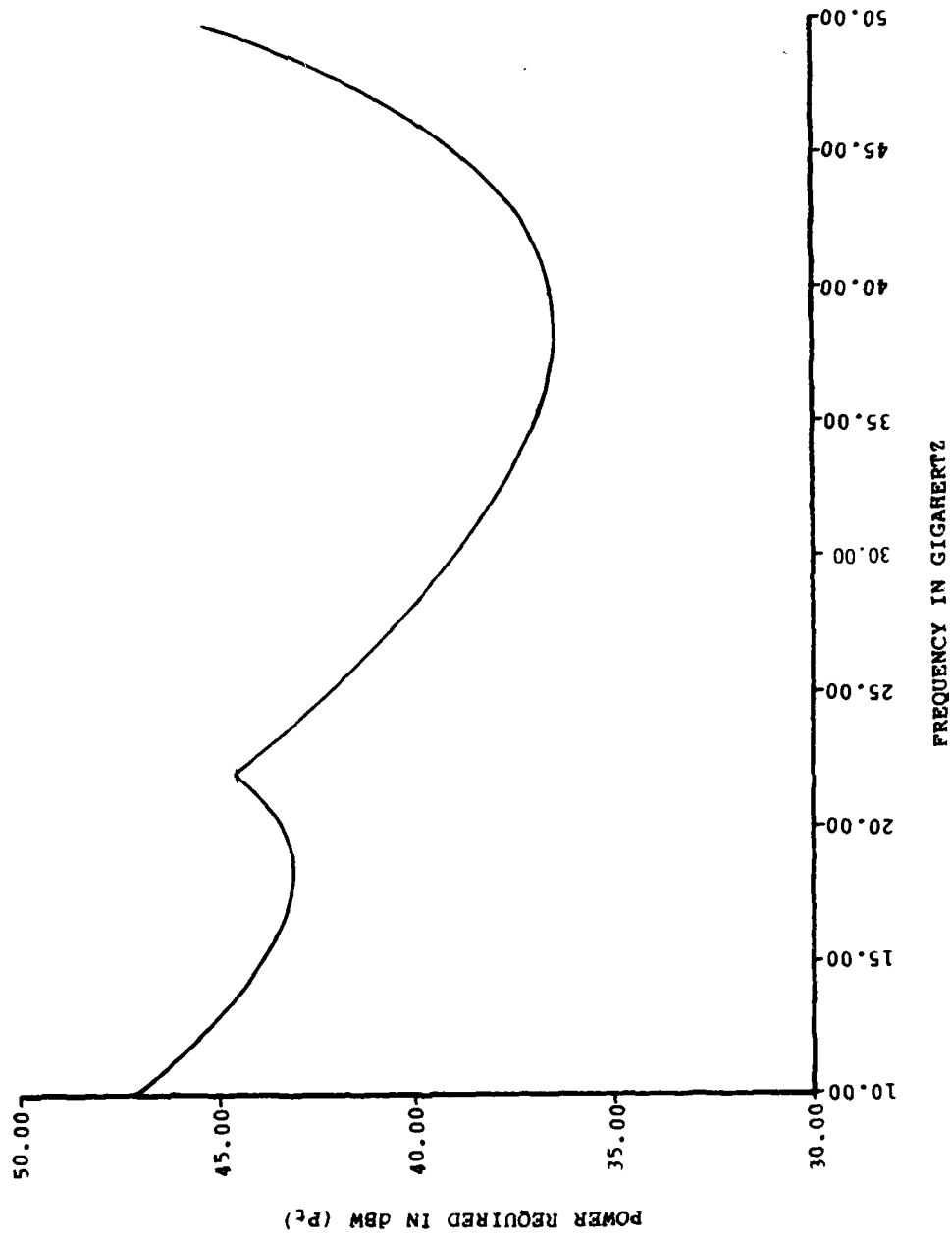


Figure 2. Transmitter power required with atmospheric attenuation.

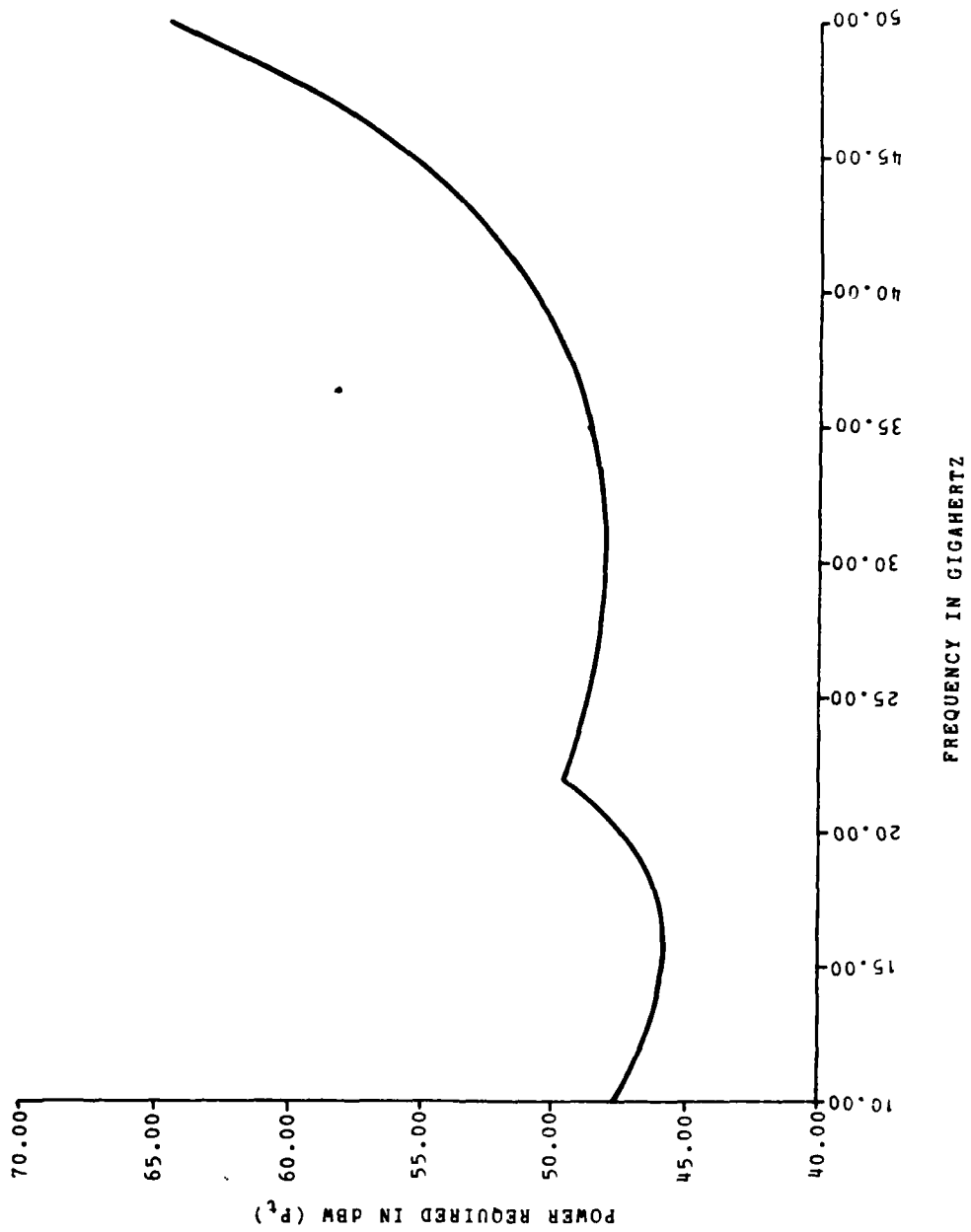


Figure 3. Transmitter power required with 4 mm of rain.

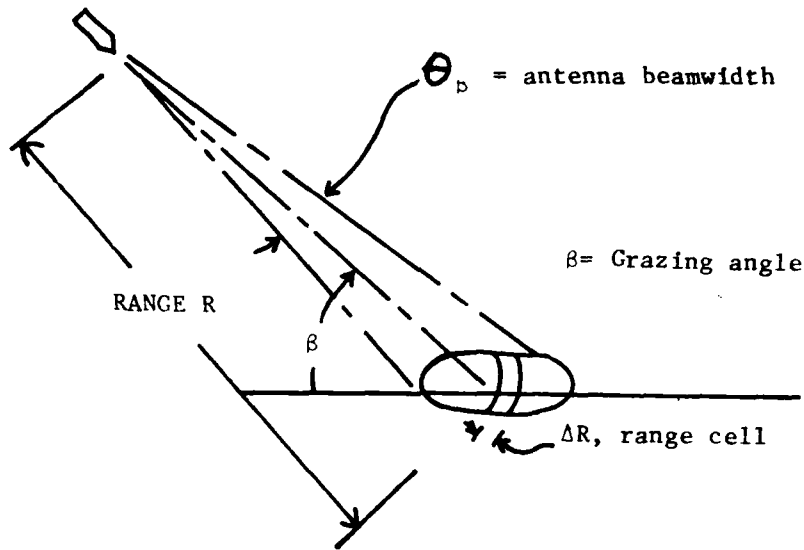


Figure 4. Clutter area.

where β is the grazing angle and D is the effective antenna diameter (meter).

The signal-to-clutter ratio becomes

$$S/C = \frac{\sigma_t}{\sigma^0 A_p}$$

$$S/C = \frac{\sigma_t f D \cos \beta}{\sigma^0 R \Delta R 3.66 \times 10^8}$$

It is generally accepted that the ground clutter is dependent on grazing angle or angle of incidence B . This dependence is commonly removed by defining a function gamma $\gamma = \sigma^0 / \sin \beta$, therefore

$$S/C = \frac{\sigma_t f D \cot \beta}{\gamma R \Delta R 1.22 c}$$

The value of gamma (γ) is constant with frequency. This point can be debated at great length, but that is not the object of this report. Nathanson¹ data show the maximum gamma for open woods to vary not more than 3 dB from L band to Ka band. The average of the median from UHF to Ka band is gamma (γ) equal to -16 dB (m^2/m^2).

¹ Fred E. Nathanson
Radar Design Principles
McGraw-Hill Book Company

Figure 5 shows the signal-to-clutter ratio as a function of frequency for three different grazing angles and $\sigma = -16 \text{ dB m}^2/\text{m}^2$, R of 5 KM $\Delta R=5$ meters. Another way to examine the same data is to plot the S/C ratio as a function of altitude (Figure 6) for various transmitter frequencies. This graphical data show the signal-to-clutter problems associated with high launch angles corresponding to high helicopter altitudes.

c. Rain Clutter

Rain and other meteorological clutter can be represented as a large number of independent scatters in a volume each with a radar cross section σ_i . The total radar cross section in a volume of the radar resolution cell V_m , therefore, can be represented as

$$\sigma_R = V_m \sum_i \sigma_i$$

The volume in a resolution cell is approximately

$$V_m \approx \pi (\theta_B R)^2 \frac{\Delta R}{8}$$

This V_m is one-half the total volume of the beam due to beam intercept with the ground.

Therefore, the signal-to-clutter ratio for rain may be expressed as

$$S/C_{\text{rain}} = \frac{\sigma_t}{\left(\frac{\pi}{8}\right) \theta_B^2 \left(\frac{c\tau}{2}\right) R^2 \sum_i \sigma_i}$$

Substituting the approximation that beamwidth θ_B is

$$\theta_B = 1.22 \frac{\lambda}{D}$$

where λ is wavelength in meters, σ_t D is effective antenna diameter in meters. and $\frac{c\tau}{2}$ is ΔR (range resolution), the S/C becomes

$$S/C_{\text{rain}} = \frac{8 \sigma_t D^2}{1.49 \lambda^2 \pi R \Delta R \sum_i \sigma_i}$$

Assuming R = 5 km, $\Delta R = 5$ meters, and antenna diameter = .1 meters, S/C becomes

$$S/C_{\text{rain}} = 1.37 \times 10^{-10} \frac{\sigma_t}{\lambda^2 \sum_i \sigma_i}$$

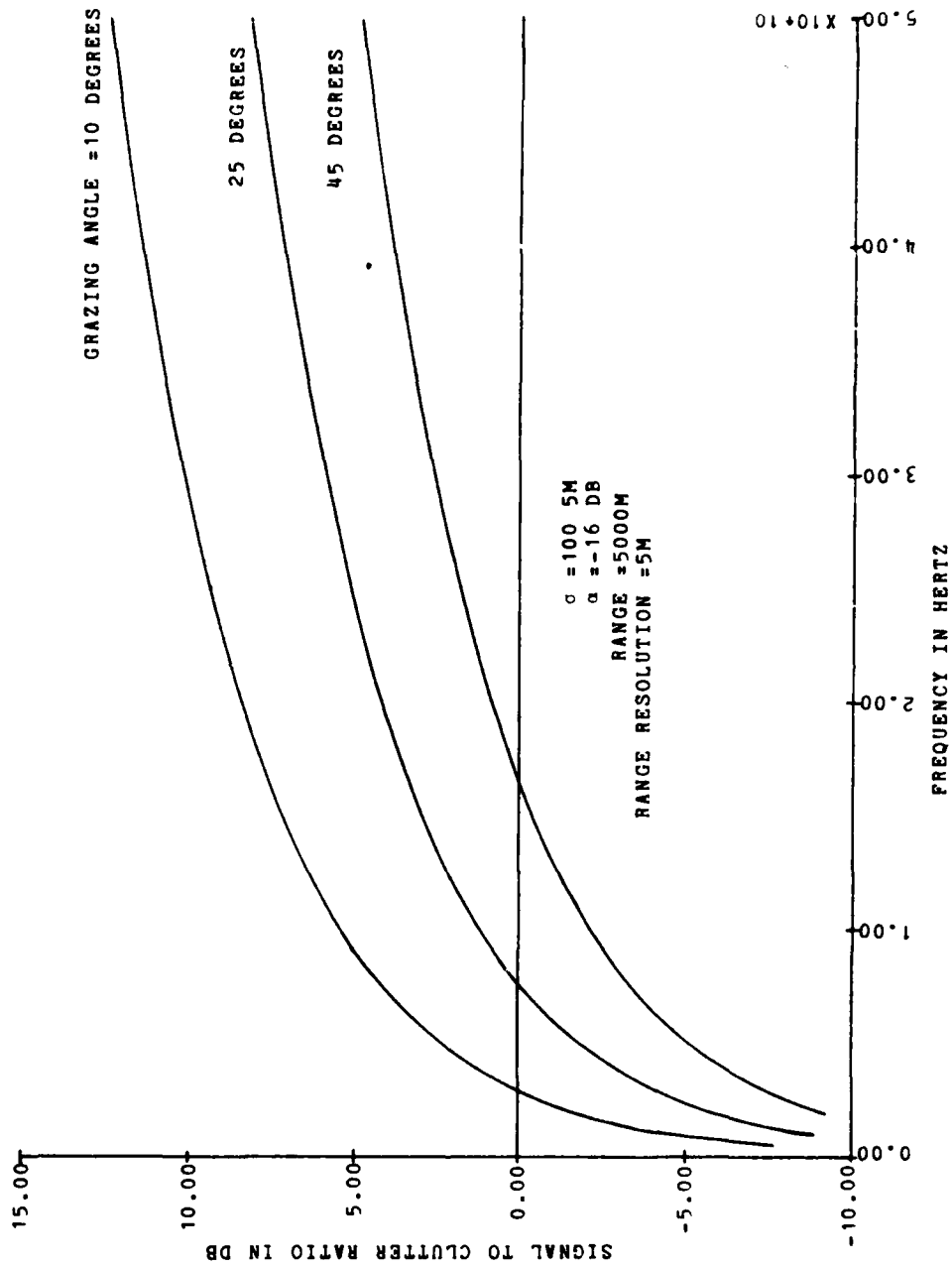


Figure 5. Signal-to-clutter ratio as a function of frequency.

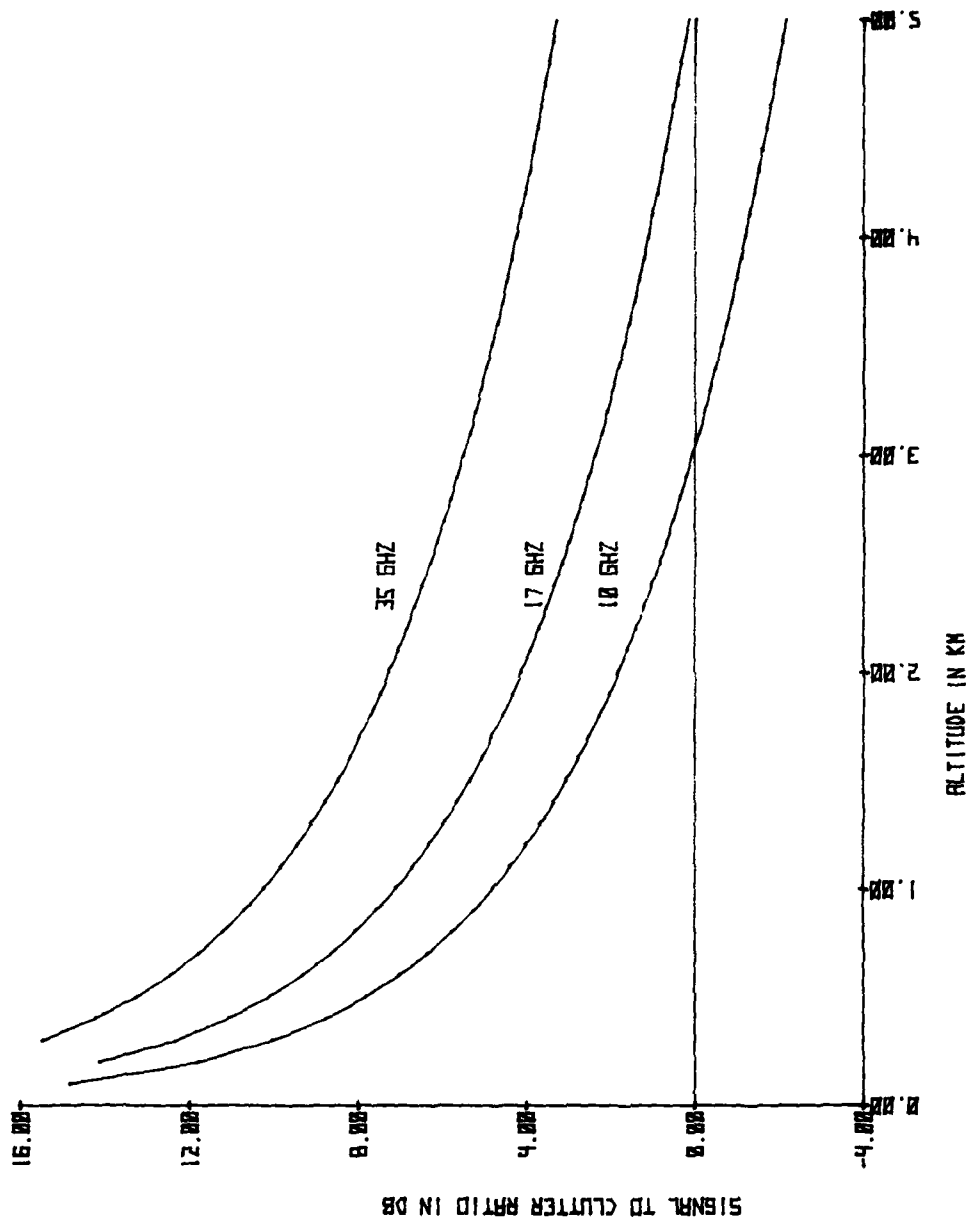


Figure 6. Signal to clutter ratio as a function of altitude.

Now replace λ with c/f and

$$S/C_{\text{rain}} = \frac{f^2 \sigma_t 1.5 \times 10^{-27}}{\sum_i \sigma_i}$$

This simple looking equation begins to cause problems when values of $\sum_i \sigma_i$ are required. It is known that $\sum_i \sigma_i$ is a function of many variables among which are drop size, frequency, and distribution or density. Drop size and density are, in turn, functions of rain rate. The reflectivity of rain is the subject of many reports. Fred Nathanson has summarized them on page 203 of Radar Design Principles, McGraw Hill Book Co., 1969. Utilizing this data and curve fitting for 4mm/hr rain, the following equation is obtained:

$$10 \log_{10} \left(\sum_i \sigma_i \right) = \frac{-62 \times 10^{3.5}}{f^{.35}}$$

$$10 \log_{10} \left(\sum_i \sigma_i \right) = -62 \times 10^{3.5} / f^{.35}$$

In Figure 7, this curve fit is compared to the data from which it was obtained. Figure 8 shows signal-to-clutter ratio as a function of frequency for $R = 5$ km, $\sigma_t = 100$ sqm, and $\Delta R = 5$ meters derived from Figure 7 and the previous signal-to-clutter without rain equation.

IV. SIGNAL PROCESSING TECHNIQUES

Feasible systems require signal-to-clutter ratios of 13 dB (20 to 1), or more, which cannot be obtained at 5 km without some signal processing to increase the nominal S/C ratio. This section will explore those techniques which are candidates for improving the signal-to-clutter ratio.

a. Synthetic Aperture Radar (SAR)

One means of reducing clutter is to narrow the antenna beam, thereby reducing the amount of clutter competing with the target. The most common procedure for reducing beamwidth is SAR, Doppler beam-splitting, or side-looking; all names describe the same process.

SAR is a natural extension of cw and pulse-Doppler radar and can be developed from these basic concepts as shown in Figure 9.

The Doppler shift frequency f_d is expressed as a function of target velocity V_r (radial) and wavelength λ .

$$f_d = \frac{2V \cos \alpha}{\lambda} = \frac{2V_r}{\lambda}$$

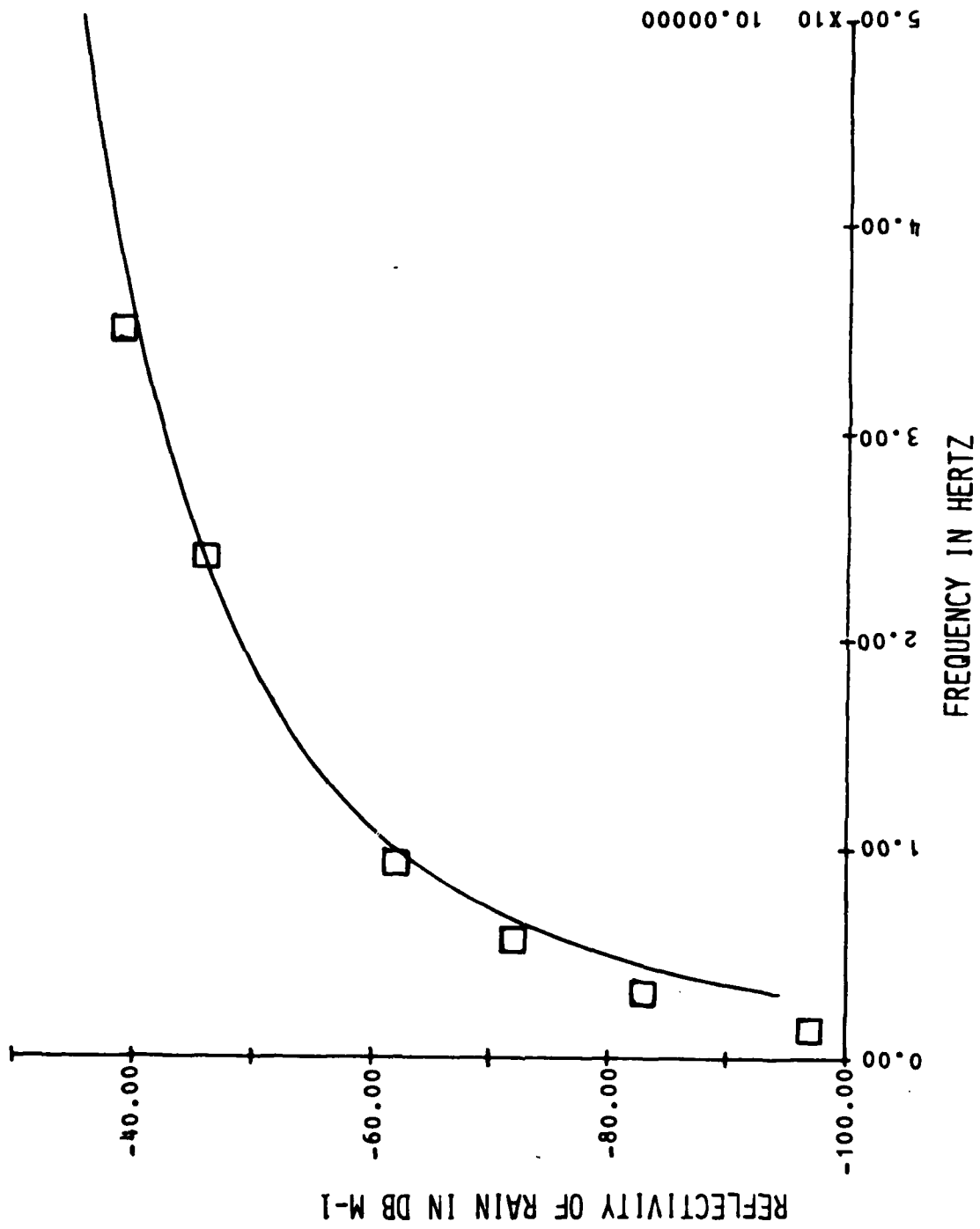


Figure 7. Reflectivity of a 4 mm/hr rain as a function of frequency.

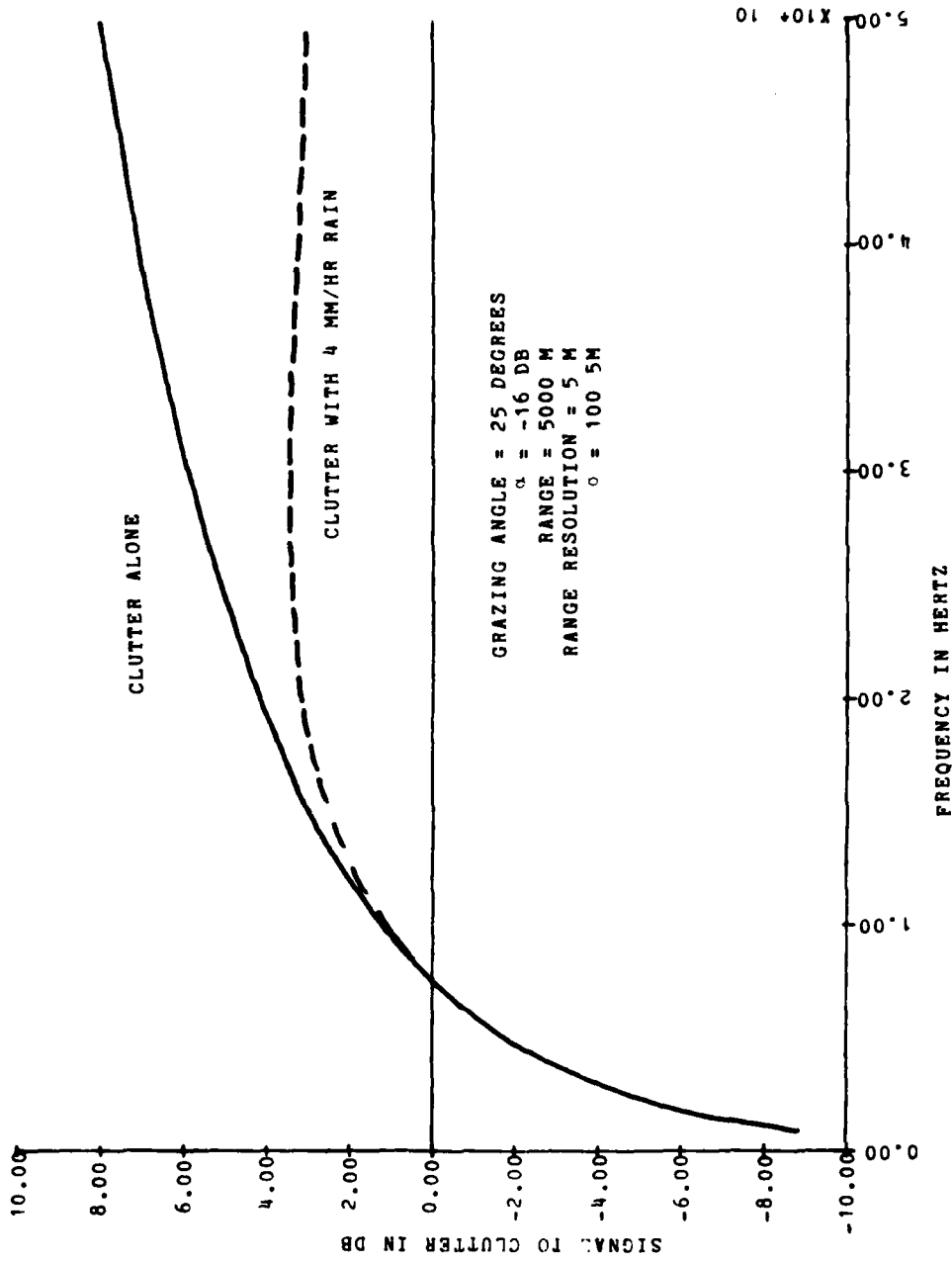


Figure 8. Signal-to-clutter as a function of frequency.

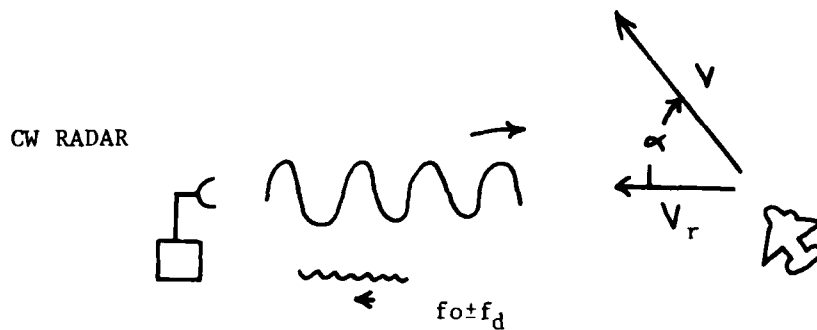


FIGURE 9. Simple CW radar.

If the roles of the target and radar are switched, i.e., radar moving and target fixed, nothing in the equation changes.

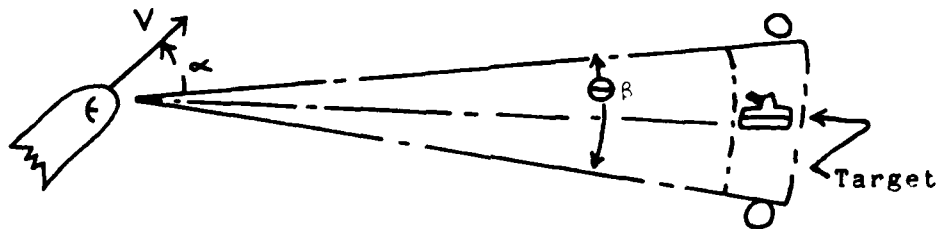


FIGURE 10. Basic missile borne radar with SAR.

The Doppler shift f_d at one side of the beam is

$$f_{d \text{ ①}} = \frac{2V}{\lambda} \cos \left(\alpha - \frac{\theta B}{2} \right)$$

and at the other side of the beam, the Doppler shift is

$$f_{d \text{ ②}} = \frac{2V}{\lambda} \cos \left(\alpha + \frac{\theta B}{2} \right)$$

Therefore, the Doppler shift across the beamwidth θB is $f_{d1} - f_{d2} = \Delta f_d$

$$\Delta f_d = \frac{2V}{\lambda} \left[\cos \left(\alpha - \frac{\theta B}{2} \right) - \cos \left(\alpha + \frac{\theta B}{2} \right) \right]$$

The factor by which the beam is narrowed and, therefore, the S/C is improved, is the improvement factor M. The improvement factor is equal to the Doppler spread across the beamwidth, divided by the final filter bandwidth, B_f

$$M = \frac{\Delta f_d}{B_f}$$

or

$$M = 2V \left[\frac{\cos \left(\alpha - \frac{\theta B}{2} \right) - \cos \left(\alpha + \frac{\theta B}{2} \right)}{\lambda B_f} \right]$$

Doppler frequency shift across the beamwidth as a function of angle off boresight is shown in Figure 11. In the case shown, the missile velocity is fixed at 200 meters/sec and the antenna diameter is fixed at 13.97 cm. Figure 12 shows Doppler shift at angles off boresight for different missile velocities. The mathematics work out such that for frequencies between 10 and 100 GHz and a constant antenna diameter, the Doppler shift (Δf) across the beamwidth is independent of radar frequency. As radar frequency increases, beamwidth narrows and Doppler frequency increases; hence, one phenomenon offsets the other.

The improvement factor that can be expected from a SAR type system is plotted in Figure 13 for a typical 16.5 GHz system with a 10-Hertz Doppler filter bandwidth and 13.5 cm diameter antenna.

b. Frequency Agile

The question of exactly what constitutes a radar target is a basic one. For general radar design purposes, targets can be equated to spherical bodies, and each is assigned some equivalent area, usually in square meters. In most cases, the typical target is somewhat larger than the wavelength of the frequency used. Thus, the effective area is some constant multiplied by the actual synthetic target size.

For evaluation of fixed frequency systems of equivalent types, this target basis does not introduce any real problem. It is obvious, however, that targets cannot be assumed to be that uncomplicated. A real target is a complex arrangement of various types of scatterers. The equivalent area becomes a statistical property which depends not only on wavelength but also on relative aspect. For two conducting elements spaced one unit apart, the amplitude of signal return will depend on the phase recombination of the re-radiated signal from these elements.

Neither can it be assumed that a target is a random spacing of simple elements. Real targets are made up of a discrete spacing of various scattering elements. The number of radiating elements activated will depend, in part, upon the wavelength of the illuminating signal. The result is an amplitude pattern for real targets which is variable with aspect. A change in illumination frequency, by affecting the scattering elements of the

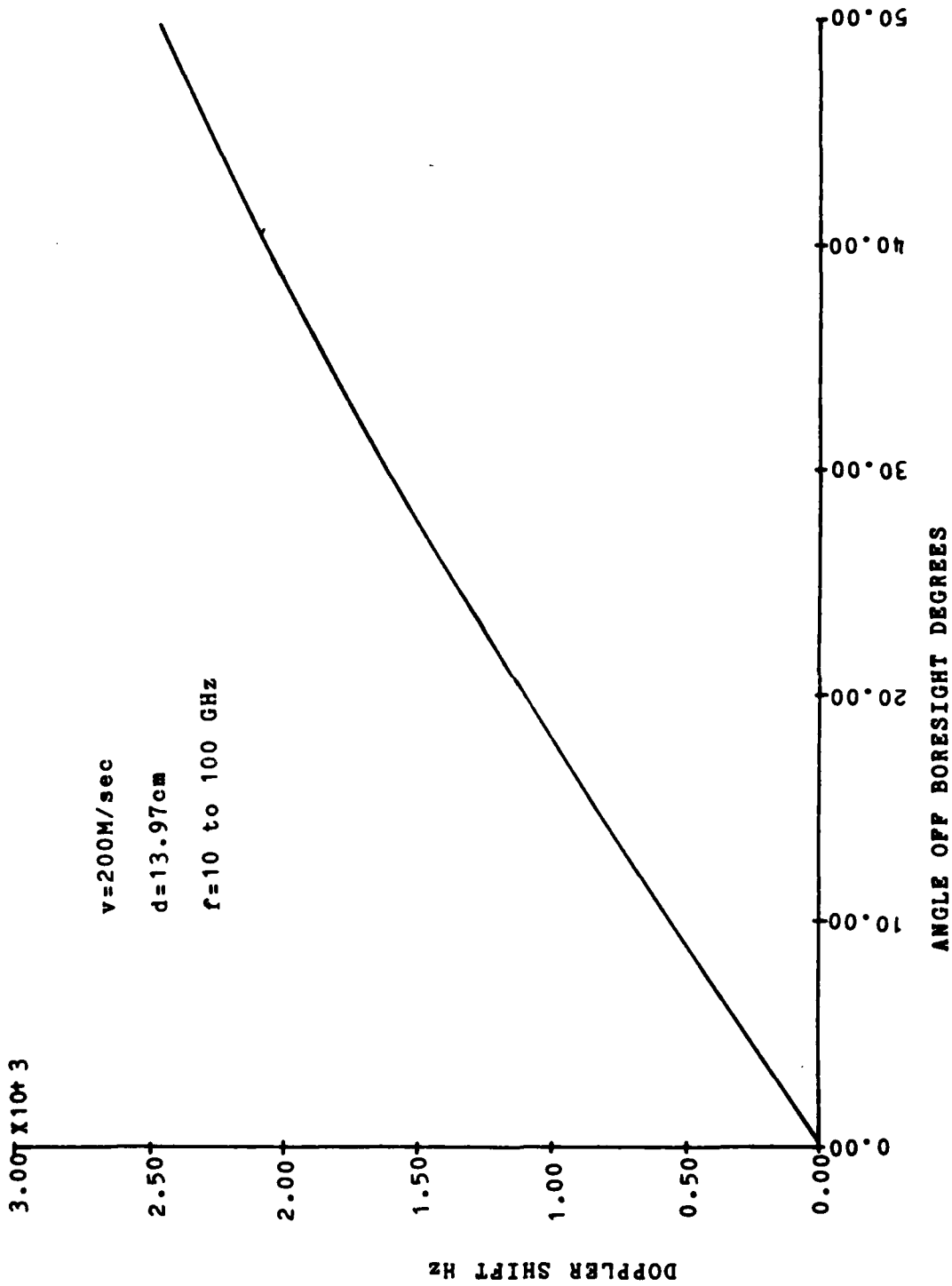


Figure 11. Doppler shift at angles off boresight.

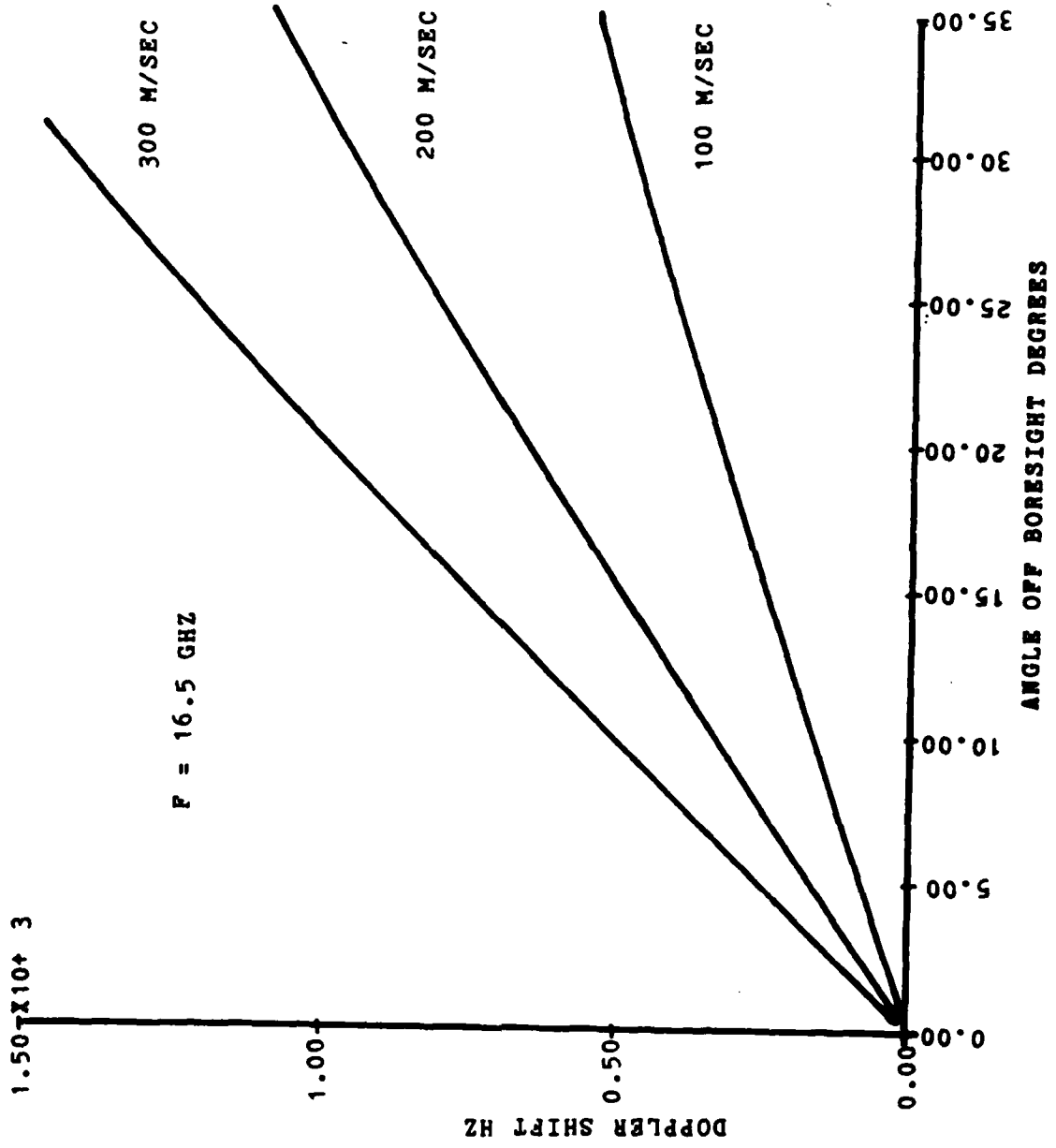


Figure 12. Doppler shift at angles off boresight for different missile velocities.

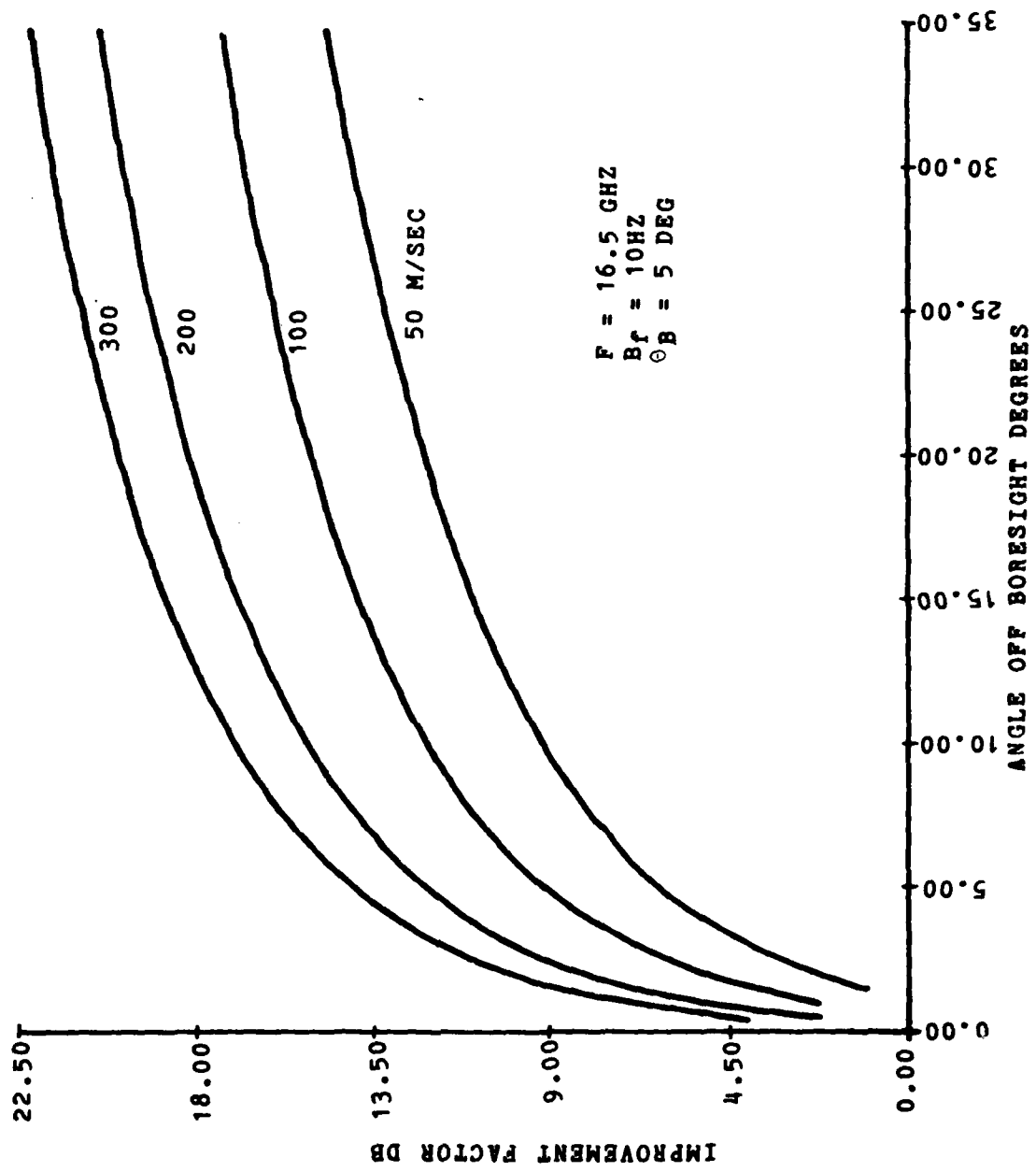


Figure 13. Signal-to-clutter improvement factor for a 16.4 GHz missile seeker.

target, produces similar amplitude fluctuations at any given aspect. To achieve optimum measure of the actual target cross-section, regardless of aspect, it would be necessary to take an average of a number of independent samples of the fluctuating return.

If frequency agility is to be used for this purpose, it would be instructive to determine the parameters Δf , transmission frequency change, and target dimensions, relative to the radar resolution cell, which relate to decorrelation (independence) of the fluctuating amplitude returns.

Generally, the amount of frequency shift necessary for decorrelation of returns from a target is a function of the characteristic range dimensions of the target complex. These dimensions can be determined by either of two factors: (1) the physical size of the target itself, or (2) the range resolution of the radar.

For the target mode, it would be necessary to have an infinite frequency change to achieve complete decorrelation. Physically, this may be justified by noting the complete randomness of the phases of the returns from the various scatterers which comprise the target complex. Because the target model assumes random spacing of the scatterers, there is a possibility of scatterers with a spacing approaching zero. Therefore, a frequency change approaching infinity would be necessary to give the required phase shift. For this reason, it is realistic to accept some finite amount of correlation as representative of the decorrelated case.

Where the target complex has a size approaching, or larger than the range resolution of the radar, i.e., extended targets like the ground in a mapping radar, the characteristic dimension D' , is generally determined by and equal to the range resolution of the system. The exact relationships of the pulse length, IF bandwidth, and video bandwidth can result in some difference between the range resolution and D' , but this does not seem significant in any practical case. Using the normal relationship that $B = \frac{1}{2\tau}$, range resolution equal $\frac{c\tau}{2}$, and the target dimension is established by the pulse length, the Δf necessary 0.5 correlation coefficient is

$$f = \frac{B}{4} = \frac{1}{3.3 \tau}$$

although the elements of the target complex may be frequency sensitive, the required change in frequency to achieve decorrelation seems to be independent of the frequency used. D' could be expressed in terms of the wavelength, with no loss of generality.

To obtain a less than 0.1 correlation coefficient it is required that f is

$$f = \frac{1}{\tau}$$

Electromagnetic backscatter obtained from radar ground mapping of complex targets usually follows a Rayleigh distribution. The Rayleigh distribution plot has a probability density function given by

$$P(x) = \frac{x}{\sigma^2} E^{-1/2 \times \frac{x}{\sigma^2}}$$

In a single frequency radar, the returned signals in one scan will fall in a very narrow band of amplitude based upon such variables as glint angle and frequency. In the next scan, the missile will have moved, the glint angle will have changed, and the signals received will fall in some other very narrow band of amplitude.

In a frequency agile radar, the amplitude of each returned signal in one scan will fall randomly on the Rayleigh probability distribution so that the signals received in one scan will be random collection of fluctuations. This collection of random fluctuation samples is averaged, resulting in the amplitude (intensity) variance being reduced by the reciprocal of the square root of the number of samples taken.

A radar ground map display will integrate the signal amplitude and display and intensity equal to the intergration of the number of pulses in a beamwidth. In a single frequency radar, the return pulses are of the same amplitude so the measurement of the significant mean value is related to a confidence factor of probability. In a frequency agile radar, each pulse varies randomly in amplitude. Therefore, a measurement of the significant mean value is related to a confidence factor of probability which has a variance reduced by one over the square root of the number of pulses.

The exact amount of signal-to-clutter improvement that can be expected is dependent upon the variation of clutter with frequency and the variation of the target with the same frequency shift. In general, this has been purported to be between 6 to 13 dB improvement; however, target discrimination techniques have been developed that exploit correlation signatures induced on radar return through the use of frequency agility.

c. Polarimetric Processing

Recent research and theory support the concept that target-to-clutter ratios are improved by using polarimetric techniques and processing.*

Man-made metallic objects, (tanks, trucks, etc.) exhibit radar return characteristics that differ from the characteristics of natural objects (earth, trees, etc.) when observed in the polarimetric domain. The radar return from metallic objects tends to exhibit strong phase lines at $+\pi/2$ or $-\pi/2$ due to the metallic surfaces forming dihedral and trihedral corner reflectors. The radar return from natural objects appears to have a more random phase. Polarimetric processing takes advantage of this difference in radar return characteristics, thereby increasing the signal-to-clutter ratio.

* Technical Report, " Analysis and Simulation of a Generic Polarimetric Radar Seeker", S.O. Dunlap, Redstone Arsenal, Ala. (In Draft)
 "Investigations of Polarimetric Processing Via Digital Simulation",
 S.O. Dunlap, Polarimetric Workshop paper, Redstone Arsenal, Al.
 June 1980

Georgia Tech Engineering Experiment Station in 1976 reported that "frequency agility or switching between horizontal and vertical polarization on a pulse-to-pulse basis induced significant amplitude modulation on the return from vegetation clutter but little modulation on the ground targets of interest."

The amount of improvement in signal-to-clutter ratio depends on the processing technique applied; therefore, each unique system must be analyzed separately.

d. Pulse Integration

In the seeker search/acquisition mode, the signal integration time is limited to the time the antenna beam scans the target of interest, or the time on target. Time on target is given by the following functional relationship:

$$T = \frac{\theta_{AZ}}{\dot{\theta}_{AZ}}$$

where

T = signal integration time or time on target

θ_{AZ} = radar azimuth beamwidth

$\dot{\theta}_{AZ}$ = azimuth scan rate

The number of pulses available for an integration per scan is given by the following:

$$P_I = PRF \cdot T$$

where

PRF = radar pulse repetition frequency

P_I = the number of pulses available for system integration

In a tracking radar, the number of pulses to be integrated can be extended. Integration may be accomplished either before the second detector or in the video. Integration that takes place in the video is called non-coherent, and integration before detection is called coherent integration. The maximum integration improvement is equal to the number of pulses integrated or

$$I = 10 \log_{10} M$$

where M is the number of pulses integrated.

e. Pulse Compression

The development of pulse compression techniques has led to an improvement factor that is theoretically equal to the pulse compression ratio so that the effective power transmitted (P) is increased by compression ratio C_r .

$$P = P_t C_r$$

The techniques for pulse compression are varied. However, the simplest form of pulse compression is linear FM which is explained in detail in Section IV a (1).

V. ELECTRONIC COUNTERMEASURES (ECM)

The parameter used to evaluate ECM performance is the received signal-to-jammer ratio (S/J) at the receiver. The use of a frequency agile radar to reduce clutter also forces the jammer to spread his power over the agile bandwidth to be effective, thus increasing his power requirements over those which would be required for radar system operating at a fixed frequency.

The signal-to-jammer power (S/J) received at the radar may be obtained from the radar range equation. The received signal power (S) is

$$S = \frac{P_r G_{rt} \sigma_t A_{rt}}{(4\pi R_t^2)^2 L_r}$$

where

P_r = transmitted radar power (effective)

G_{rt} = power gain of radar antenna in the direction of the target

σ_t = target radar cross section

A_{rt} = effective area of the radar antenna in the direction of the target

R_t = slant range from radar to target

L_r = radar losses; not including atmospheric losses

Similarly, the jammer power received in the receiver bandwidth is

$$S = \frac{P_j G_{jr} A_{rj} B_r}{4\pi R_j^2 L_j B_j}$$

where

- P_j = transmitted jammer power
- B_j = total bandwidth to be jammed (frequency agile bandwidth)
- P_j = jammer power per unit bandwidth
- $J_0 = \frac{P_j}{B_j}$ = jammer power per unit bandwidth
- G_{jr} = power gain of jammer antenna in direction of the radar
- A_{jr} = effective area of radar antenna in the direction of the jammer
- B_r = receiver instantaneous bandwidth
- R_j = slant range from jammer to radar
- L_j = jammer losses; not including atmospheric losses

The single pulse S/J may be written as

$$(S/J)_1 = \frac{P_{rj} \sigma_t A_{rt} R_j^2 L_j G_{rt}}{J_0 G_{jr} A_{rj} 4\pi R_t^2 L_r B_r}$$

Assuming the following parameters

- P_r = 1.0 kilowatt (effective)
- G_{rt} = 32 dB = 1.585×10^3
- B_r = 20 MHz

The target radar cross section is taken to be 100 m^2 and the loss ratio L_j/L_r (not including propagation loss) will be assumed equal to one. The single pulse S/J (excluding propagation losses) is then

$$(S/J)_1 = \frac{0.6306}{J_0} \left[\frac{1}{G_{jr}} \right] \left[\frac{R_j}{R_t} \right] \left[\frac{A_{rt}}{A_{rj}} \right]$$

where J_0 is the jammer power density in watts/Hz and R_j and R_t are in units of meters. For a jammer located in the vicinity of the radar ($R_j = R_t$) radiating into the radar antenna sidelobes the ratio becomes

$$(S/J)_1 = \frac{0.6306 G_{s1}}{J_0 R^2 G_{jr}}$$

G_{jr} is the gain of the jammer antenna in the direction of the radar and G_{s1} is the ratio of maximum to sidelobe level gains for the radar antenna.

Figure 14 shows the single-pulse signal-to-jammer ratio under the conditions of a sidelobe jammer with unity gain in a 30 dB sidelobe, 20 dB sidelobe and in the main beam ($G_S = 1$). These curves do not consider the gain from any integration of pulses.

VI. RADAR ERRORS

Errors encountered in radar measurement can be classified as either noise (random) or bias (fixed). These types of errors are contained in the three measurements most often made with a radar (1) range-to-target, (2) the rate of change of range (doppler), and (3) the angle of arrival. This section will examine the effect of both noise and bias errors on these three basic measurements.

a. Range Errors

There are few techniques that can duplicate the ability of a radar to determine range to a distant object in most all weather conditions. The measurement of range is the measurement of the time difference between a suitable reference signal and the arrival of the echo signal. The reference signal is usually the transmitted signal.

(1) Thermal Noise

In radar, range is determined by measuring the time required for the wave front to reach the target and be returned.

$$t_R = \frac{2R}{c}$$

where

R is the range of the target

C is the velocity of light

t_R is the time required to travel to the target and back.

A method of range measurement is to measure the time (t_r) at which the leading edge of a returning wave or pulse crosses some threshold. This pulse is not precisely rectangular, but has rise times and decay times, plus some noise. The effect of the noise is to distort the shape of the pulse and change threshold crossing time (t_r), Figure 15.

In the case of large signal-to-noise ratio, the maximum slope of pulse is A/t_r , where A is the pulse amplitude and t_r is the rise time. The slope of the noise is the ratio of noise voltage in the vicinity of the threshold crossing $[n(t)]$ to the error in time measurement (Δt_r). Because of the large signal-to-noise ratio, the two slopes are essentially the same. Equating the two expressions gives:

$$\Delta t_r = \frac{t_r}{A/n(t)}$$

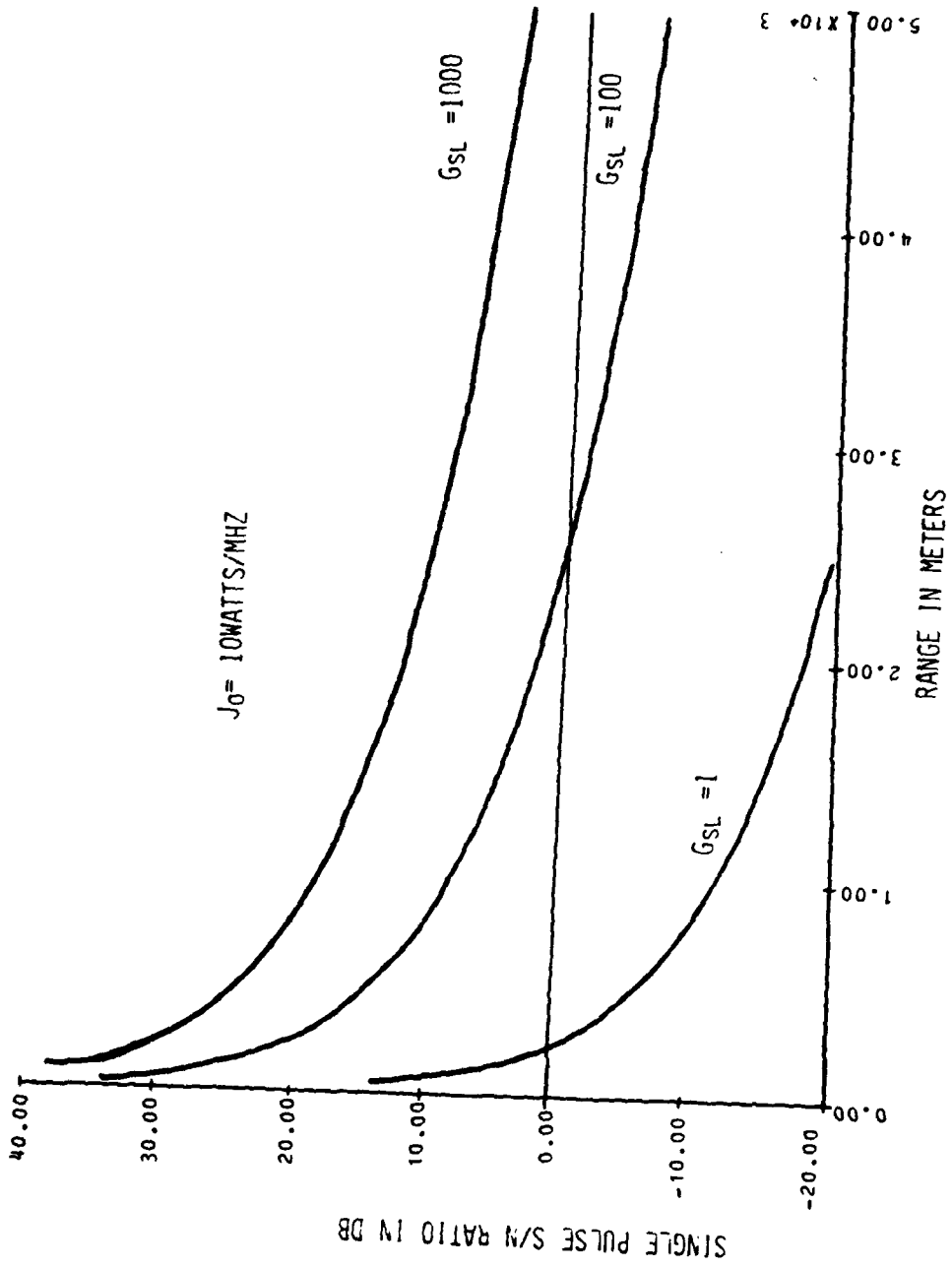


Figure 14. Single pulse signal-to-jammer ratio as a function of range - no propagation loss.

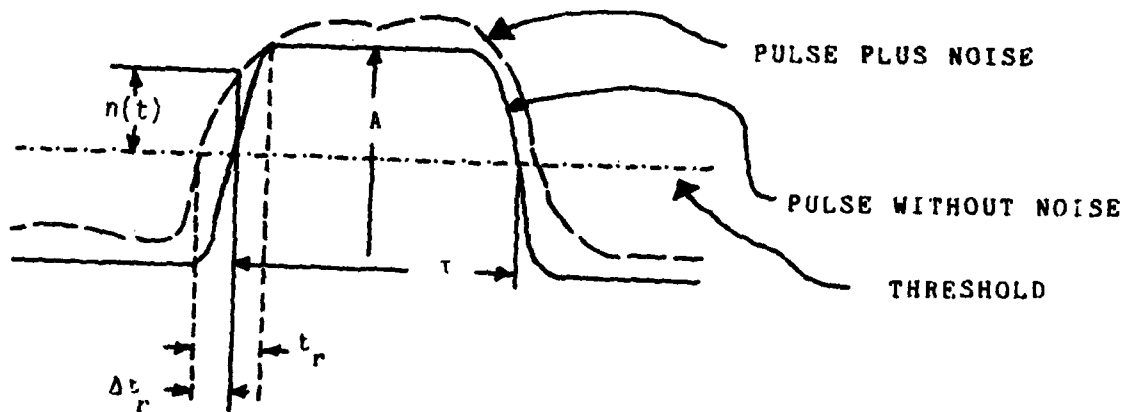


Figure 15. Radar pulse shape.

The root-mean-square value

$$St_r = \sqrt{(\Delta t_r)^2} = \frac{t_r}{\sqrt{\frac{A^2}{\bar{n}^2}}}$$

where

$\frac{A^2}{\bar{n}^2}$ is the video signal-to-noise power ratio:

$$\frac{A^2}{\bar{n}^2} = 2 \frac{S}{N}$$

follows from the idea that video signal-to-noise power ratio is equal to twice the intermediate frequency (IF) signal-to-noise power ratio (S/N), assuming a square-law linear detector and, once again, a large signal-to-noise ratio.

Rise time (t_r) is a function of bandwidth (B) of the IF amplifier. Then

$$t_r = \frac{1}{B}$$

Using the above, (δt_r) can be rewritten as

$$\delta t_r = \frac{1}{B \sqrt{2 \frac{S}{N}}}$$

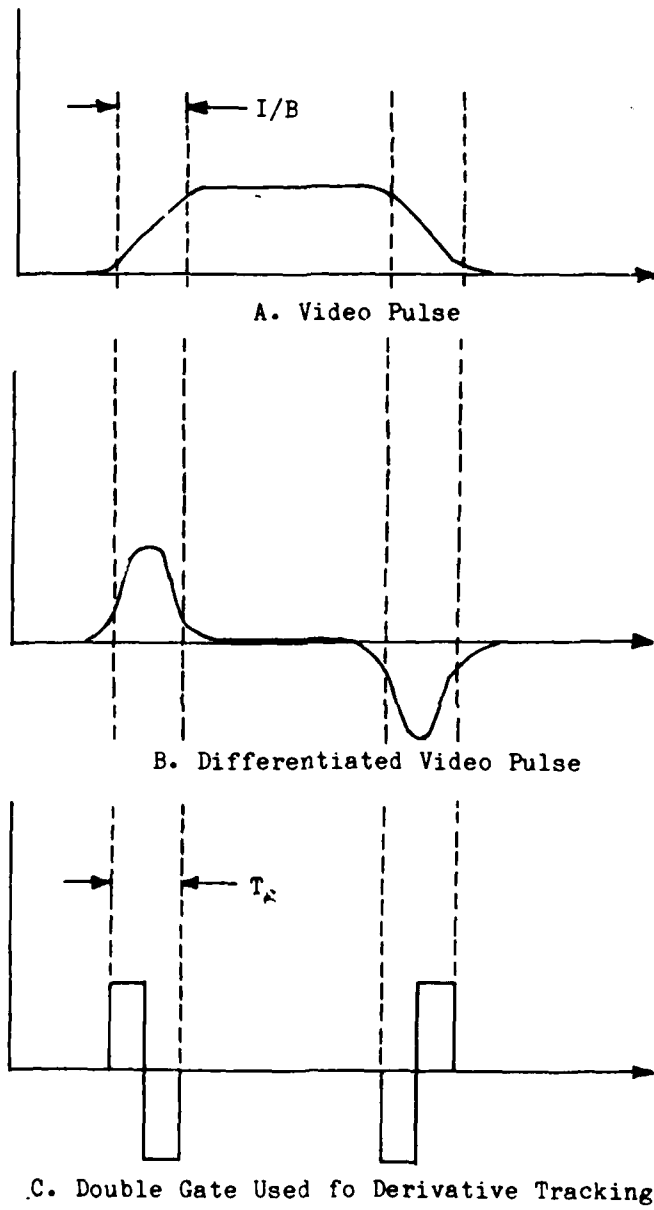


Figure 16. Leading and trailing edge tracker.

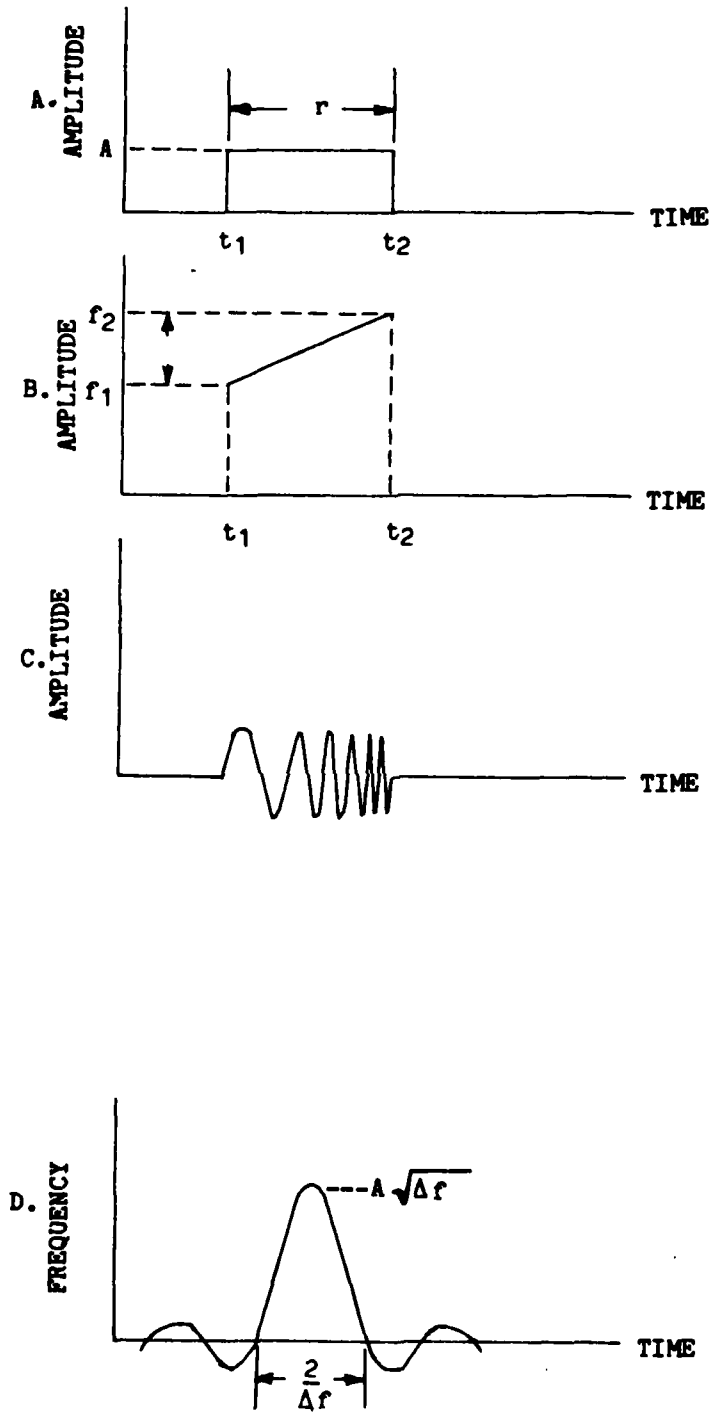


Figure 17. Frequency-modulated pulse-compression wave forms.

If an independent measurement could be made on the trailing edge and the rise time and decay time are equal, the result of the two combined measurements would be

$$\delta t_r = \frac{1}{B \sqrt{4 \frac{S}{n}}}$$

The range error in units other than time can be obtained using the relationship

$$\delta R = \frac{C \delta t_r}{2}$$

therefore,

$$\delta R = \frac{C}{2B \sqrt{4 \frac{S}{n}}}$$

assuming combined leading and trailing edge tracking.

One of the more simple methods of leading and trailing edge tracking is to use two narrow gates, each of width equal to the rise time of the pulse and separated by an amount equal to the pulse width (Figure 16). Tracking becomes the simple matter of keeping equal energy of the split tracking gates (τ_g) in Figure 16c.

Pulse compression (linear frequency modulation) is a special case of the pulsed radar. The transmitted waveform consists of a rectangular pulse of constant amplitude (A) and duration (τ) (Figure 17A). The frequency (f) of the transmitted pulse (Figure 17B) increases from f_1 to f_2 over the duration of the pulse. The time waveform of a signal having the properties described by Figures 17A and 17B is shown schematically in Figure 17C. Upon being received, the echo is passed through the pulse compression filter, which is designed so that the velocity of propagation through the filter is a function of frequency. In this example, the filter must delay the higher frequencies at the trailing edge of the pulse less than the delay of the lower frequencies at the leading edge. The result is that the energy contained in the original long pulse of duration is compressed into a shorter pulse of duration approximately defined by the inverse of the change in frequency, or $1/\Delta f$, where $\Delta f = f_2 - f_1$. The shape of the pulse is proportional to $(\sin \pi \Delta f \tau) / (\Delta f \pi \tau)$. The instantaneous peak power of the original pulse is theoretically (all systems have some loss) increased by the factor $(\Delta f \tau)$; pulse amplitude is increased by $\sqrt{\Delta f}$ (Figure 17D).

The method used to determine the time error (δt_r) for rectangular pulse can be used to find the time error for a compressed pulse. The results are the same as replacing the bandwidth term with the frequency change (Δf), and increasing the signal amplitude by $\sqrt{\Delta f \tau}$.*

The development is as follows. The slope of pulse in noise is (see Figure 18):

$$\frac{n(t)}{\Delta t_r}; \quad S/N > 10.$$

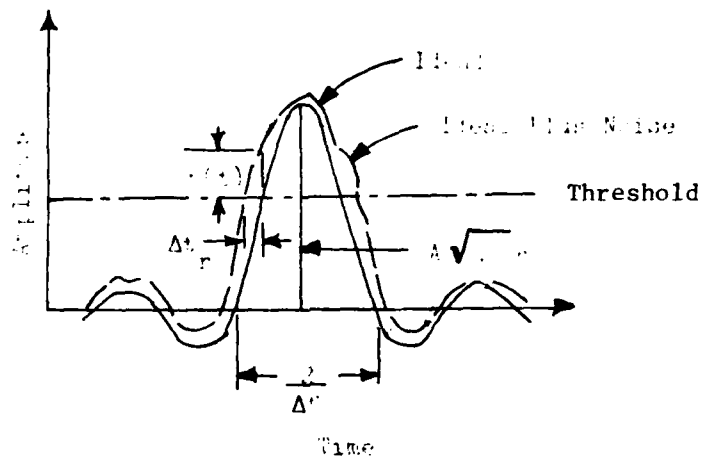


Figure 18. Compressed pulse with noise.

where

A is peak amplitude of compressed pulse

Δf is linear frequency shift during transmission
($\Delta f = f_2 - f_1$)

$n(t)$ is the noise voltage at the threshold

Δt_r is the error in the time-delay measurement.

The slope of pure or ideal pulse may be approximated as

$$\frac{2 A \sqrt{\Delta f \tau}}{2 \Delta f} = A \Delta f \sqrt{\Delta f \tau}; \quad \Delta f \tau > 10$$

* D.K. Barton, Radar System Analysis, Prentice Hall, Inc., Englewood Cliffs, New Jersey (1964), p. 47.

Equating the two slopes and solving for Δt_r gives

$$\Delta t_r = \frac{n(t)}{A\sqrt{\Delta f}} \Delta f = \frac{1}{\Delta f A\sqrt{\Delta f \tau} / n(t)}$$

or

$$\sqrt{(\Delta t_r)^2} = \frac{1}{\Delta f \sqrt{2 s/n} \sqrt{\Delta f \tau}}$$

Using trailing edge to make another measurement of range,

$$\delta t_r = \frac{1}{2 \Delta f \sqrt{s/n} \sqrt{\Delta f \tau}}$$

The equation developed for the error in time delay for a pulse compression radar is an approximation, because the slope of the pulse is treated as a triangle instead of $\sin x/x$ shape; another solution can be obtained by evaluating the equivalent bandwidth (β)*

where

E is total energy in the pulse

N_0 is the noise per cycle bandwidth

β is the equivalent bandwidth

$$\beta = \frac{\pi \Delta f}{\sqrt{3}} \quad \text{when } \Delta f \tau \gg 1.$$

Therefore, δt_r becomes

$$\delta t_r = \frac{\sqrt{3}}{\pi \Delta f \sqrt{2 E/N_0}}$$

* M.I. Skdnik, Introduction to Radar Systems, McGraw-Hill Book Company, New York (1962), p. 496.

in order to account for the pulse widening that occurs when "weighting" is used to reduce the time of range sidelobes, a factor (K_w) is multiplied by the range error equation. This pulse widening factor is near unity; as typical examples, a Taylor weighting function has a $K_w = 1.41$; a cosine-squared function, 1.62; a Hamming function, 1.47. Therefore, the final form of the noise range error is

$$\delta t_r = \frac{\sqrt{3} K_w}{\pi \Delta f \sqrt{\Delta f \tau} \sqrt{2 s/n}} \quad \text{sec}$$

or

$$\delta R = \frac{\sqrt{3} K_w 3 \times 10^8}{2\pi \Delta f \sqrt{\Delta f \tau} \sqrt{2s/n}} \quad \text{meters}$$

(2) Multipath

The surface of the earth has some reflectivity (ρ) that causes an error to be introduced as a result of multipath reflections. Figure 19 shows the cause of multipath errors.

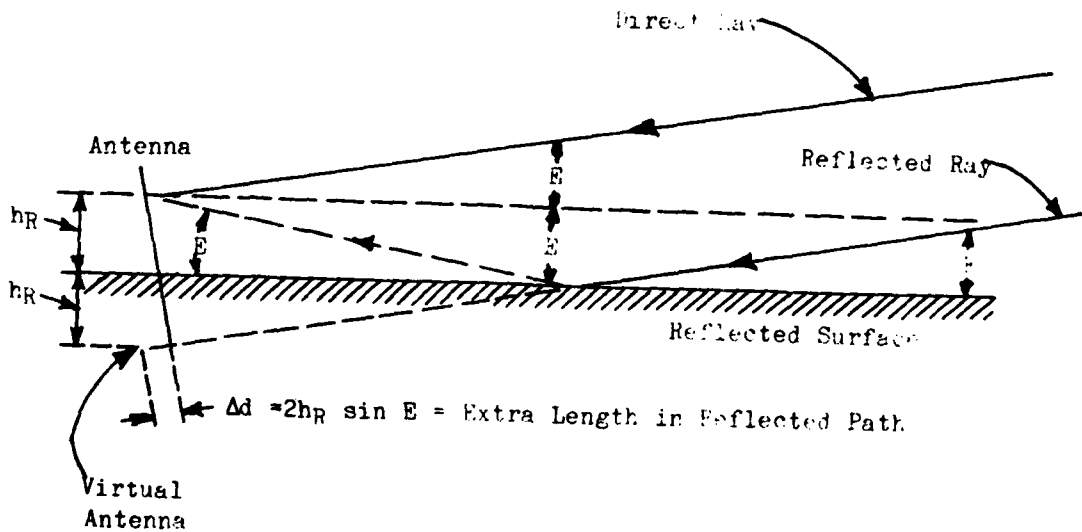


Figure 19. Range multipath errors.

If the height of the radar above the surface is (h_R) and the elevation angle of the tracked target is (E), the expression for the difference in range between the direct return and the reflected or multipath return (Δd) is

$$\Delta d = 2 h_R \sin E$$

The two range components will have a phase difference (ϕ), due to the added length of the path traveled by the reflected ray of:

$$\phi = \frac{4\pi h_R}{\tau} \sin E \quad (\text{radians}).$$

The signal voltage of the direct ray (V_D) will be proportional to the antenna gain (G_D).

$$V_D = K \sqrt{G_D}$$

The reflected ray will have a signal voltage (V_R) proportional to the gain of the antenna (G_R) at some angle off the target boresight ($2E$).

$$V_R = \rho K \sqrt{G_R}$$

where

ρ is the surface reflectivity of the earth, always less than unity. The ratio of V_D to V_R is

$$\frac{V_D}{V_R} = \frac{1}{\rho} \sqrt{\frac{G_D}{G_R}}$$

The root-mean-square range error due to multipath becomes

$$\sigma_{rms} = \sqrt{2} \rho h_R \sin E / \sqrt{\frac{G_D}{G_R}}$$

G_D/G_R is the power ratio of the target antenna gain at boresight to the reflected target antenna gain off boresight (see Figure 20 for an example).

Figure 21 shows how multipath reflections cause range errors due to the direct and reflected ray combinations within the range gate. The maximum value of $h_R \sin E$ that permits reflected energy to enter the range gate is approximately equal to the pulse width of the radar, so that the limit to the multipath range error (σ_{rms}) is

$$\sigma_{rms} = \frac{\tau}{2 \sqrt{G_D/G_R}}$$

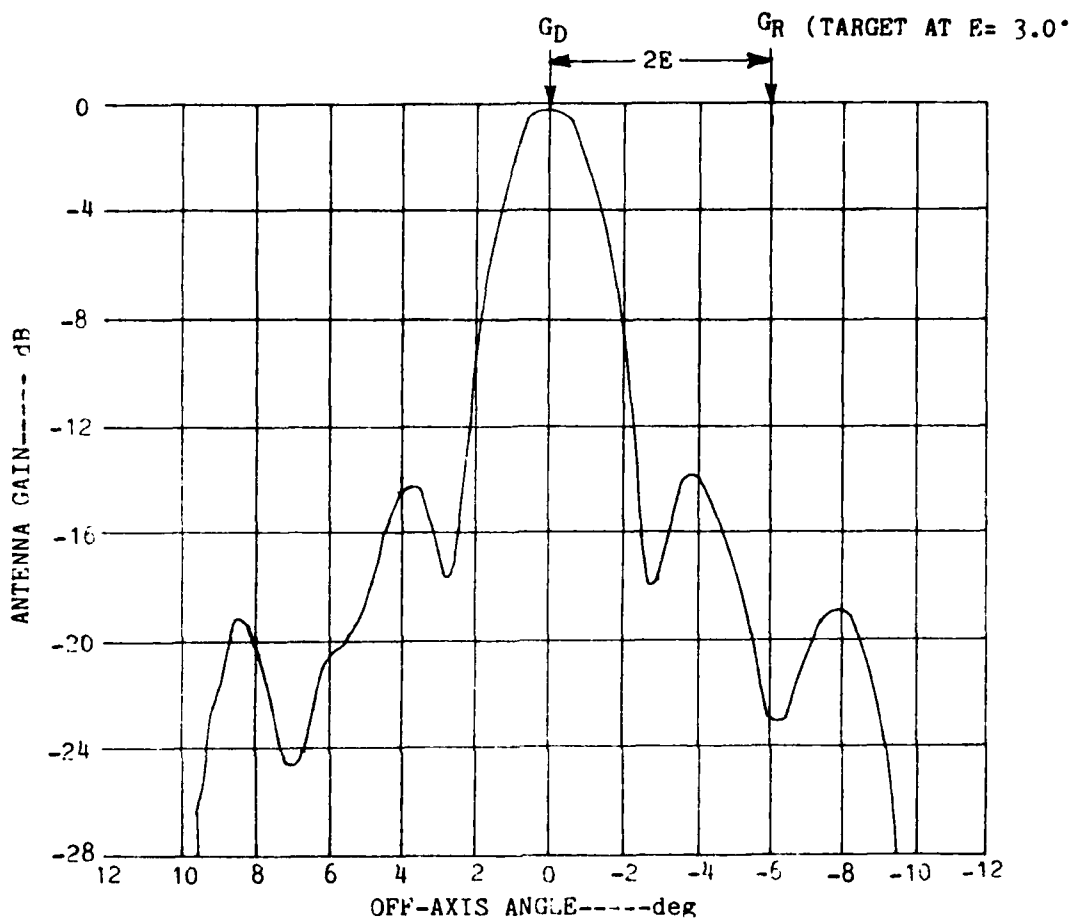


Figure 20. Typical antenna pattern for multipath (elevation).

The multipath range error is usually small; e.g., if the reflected ray is 20 dB off the main lobe and the earth is 100% reflective, σ_{rms} will only be $\tau/20$ as a maximum.

(3) Frequency Oscillator

In a tracking radar, the usual frequency standard consists of a crystal-controlled oscillator operating in a temperature-controlled, vibration-free chamber. At most locations where precision radars may be used, it is relatively easy to assure an accuracy in time-interval measurement within one part in 10^9 . An accuracy within one part in 10^8 can be maintained over an indefinite period, even at remote locations on the earth.

Once the local frequency standard has been established, conventional techniques of frequency multiplication and synthesis may be used to obtain signals at any frequency up to the transmission frequency of the radar. These frequencies, in turn, are available to control the generation of measurement of internal time delays, with almost the same accuracy as the frequency standard. The error due to the frequency standard in a digital ranging system can be less than 1 foot.

(4) Converter and Quantization Noise

In a real-time signal processor, the analog-to-digital (A-D) converter must operate extremely rapidly. Rates up to 1 MHz are typical. At the same time, it is desirable to quantize the sample to perhaps 10 bits. The effort to produce more and more bits of resolution may result in the last bit being a random variable reflecting internal noise in the circuits and power supplies rather than signal levels. The uncertainty of this last bit is converter noise and is a function of the A-D conversion.

(5) Internal Jitter

The radar transmitter pulses are triggered by the local frequency standard. In a practical radar system, there is a degree of uncertainty about exactly when the pulse is generated. The variation in start time of pulses is known as internal jitter.

(6) Receiver Delay

The signal delivered to the range tracker will be delayed by the passive radio frequency (RF) elements as well as active RF and intermediate frequency (IF) amplifier stages of the receiver. The major portion of this delay is bias, and can be removed in the initial calibration of the system. Other portions are temperature sensitive, and may be held within tolerances by temperature control. The delay caused by the IF amplifier is a function of tuning and signal strength. Errors of this type can be minimized by use of RF attenuation or by calibration of delay as a function of signal strength. Relative errors in receiver delay can usually be maintained at values representing less than 1 foot.

(7) Range Glint

The fact that two or more targets or scatters on a large single target can appear in a resolution cell causes a noise error in range that is independent of the range to the target. This error is closely related to the multipath problem discussed in Section XIa (2) where the radar sees the target plus its blurred image reflected from the surface. If the multipath signal in Figure 21 is considered to be a return from another target or scatter, as the case may be, the same results would be a qualitative effect of target range glint.

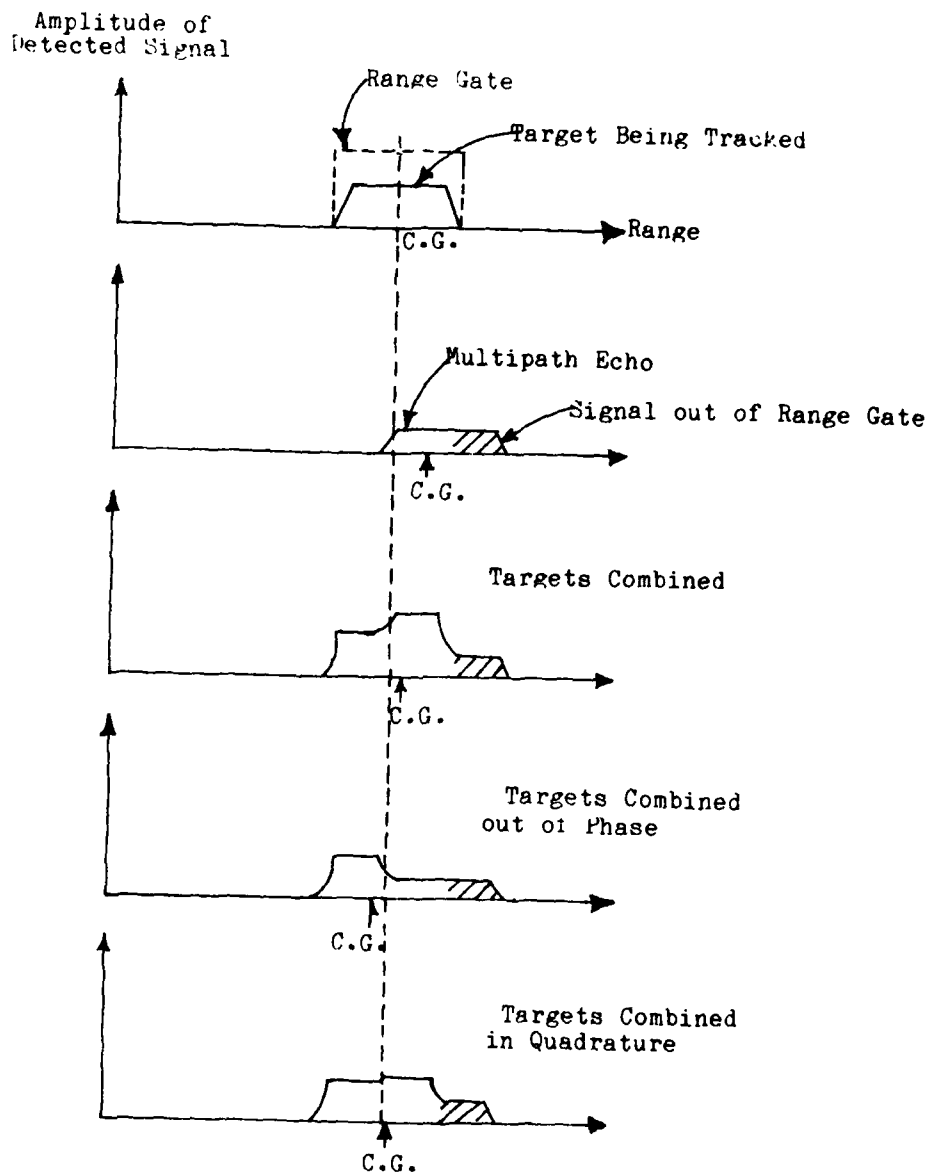


Figure 21. Radar errors due to multipath.

The root-mean-square (rms) error associated with range glint (σ_r) is dependent on the length of the target parallel to the radar ray and results from assuming that a target consists of scatters distributed uniformly along the radial target length (L_r).

$$\sigma_r = K_g L_r$$

where

K_g is a constant varying from 0.2 to 0.35.

b. Angle Errors

In addition to their grouping as noise and bias errors, the errors associated with angles fall into two other categories: azimuth and elevation. In general, any error that applies to elevation applies also to azimuth, but not under all circumstances. In this discussion, any difference between azimuth and elevation will be pointed out; otherwise, angle errors will be assumed to be applied equally to azimuth and elevation.

Because angle tracking can be obtained in many ways to obtain an angle position, an introduction to these methods is presented here. The error involved with each method may also differ, and when not otherwise specified, these errors apply equally to all methods of angle tracking.

(1) Sequential Lobing

A technique used early in radar tracking is sequential lobing which is switching the antenna from one side to the other of the tracked target. The amplitude of the returns will be equal when the target is boresighted between the switched positions of the antenna. If the target is not boresighted, the difference in amplitude is the error signal.

(2) Conical Scanning

A natural extension of the sequential lobing technique is conical scanning. Instead of switching antenna positions continuously, a beam is rotated around the target being tracked. If the target is in the boresight of the rotation beam, the returns are of equal amplitude. If the target is not on boreline, the resulting modulated signal can be used as an error signal to adjust the antenna position. Conical scanning and sequential lobing have another characteristic in common, i.e., both require more than one pulse to determine position. To obtain both elevation and azimuth angles, a minimum of three pulses is required.

(3) Monopulse

The previous tracking methods described require more than one pulse to determine angle. If the tracked target did not fluctuate between pulses

the system would be ideal, but targets do change in amplitude and phase from pulse-to-pulse because of changes in radar cross section. These pulse-to-pulse fluctuations of the echo signal would have no effect on tracking if angle measurement was extracted from one pulse. This one-pulse angle tracking technique can be applied in several ways and the general case is known as monopulse.

Monopulse is achieved by generation of multiple antenna beams per pulse and extracting angle information from a single pulse in the multiple beams. In general, a cluster of four feeds is used to obtain both elevation and azimuth error signals. In a phased array, monopulse can be achieved by either amplitude or phase comparison, depending on the feed technique. A feedthrough or space-feed array acts as an RF lens, and a reflection-array acts like a parabolic reflector. Monopulse angle-error sensing can be accomplished in a corporate-feed array by using halves of the array (the top and bottom halves are used for elevation); left and right halves are used for azimuth.

(4) Thermal Noise

The ability of a radar to determine the angle of arrival of a phase front is limited by the noise in the system as well as other factors such as polarization, as was the case with range measurement.

The root-mean-square (rms) associated with a monopulse tracking system (σ_1) is expressed by:

$$\sigma_1 = \frac{\theta_b}{k_m \sqrt{2 s/n}}$$

where

θ_b is antenna beam width

k_m is error slope or the slope of the monopulse error curve at a zero angle ($1.2 < k_m < 1.6$)

S/N is signal-to-noise power ratio on axis

If the angle tracking is done within a range gate and averaged over a pulse width (τ), then the error becomes

$$\sigma_1 = \frac{\theta_b}{k_m \sqrt{2B \tau (s/n)}}$$

(filtered by $B\tau > 1$)

where

B is the IF bandwidth

τ is the pulse width

Monopulse tracking systems can be broken into two groups: beam-pointing and off-axis. In the beam pointing monopulse, the antenna is continuously pointed at the target to keep it on axis. The off-axis monopulse points the beam in the general direction of the target and measures the angle by the beam direction and error voltage, whereas the beam pointer strives to keep the error at zero. Previous equations apply to the beam pointing case. The root-mean-square error for off-axis monopulse tracking is expressed by:

$$\sigma_{\theta} = \frac{\theta_b \sqrt{L_{\theta} \left[1 + \left(\frac{k_m \theta_t}{\theta_b} \right)^2 \right]}}{k_m \sqrt{2 S/N}}$$

where

L_{θ} the ratio of the antenna gain on-axis to the gain off-axis

θ_t is the angle of the target off-boresight or boreline, where boreline is the pointing direction [not to be confused with scanning angle, which refers to an angle off a fixed direction (broadside)]

S/N is the single-pulse signal-to-noise ratio on axis

Tracking by the off-axis method allows the introduction of a bias error from improper calibration of the error curve at the selected gain setting. Because this off-axis tracking error is greater than the on-axis or beam pointing error by a factor of

$$\sqrt{L_{\theta} \left[1 + C k_m \theta_t / \theta_b^2 \right]},$$

it is normally used in angle measure in search mode only and not for precision tracking.

The rms thermal noise angle error (σ_c) in a conical scanning system is given by

$$\sigma_c = \frac{\theta_b \sqrt{2 L_k}}{K_s \sqrt{2 (s/n) (B\tau) \left(\frac{f_r}{B_n}\right)}}$$

where

L_K is the crossover loss due to the off-axis tracking as the beam rotates around the target

k_s is the error slope similar to that for monopulse (k_m) in Paragraph XIb (4) conical scanning sensitivities usually lie 40% to 80% below k_m .

S/N is the maximum or on-axis signal-to-noise ratio

f_r is the pulse repetition frequency

B_n is the servo bandwidth

B is the receiver bandwidth

τ is the pulse width.

(5) Multipath

The earth's surface reflectivity (ρ) that causes multipath range errors also causes angle errors due to the two signals arriving from different angles. The source of angle multipath errors was explained in section XIa (2).

The rms angle error due to multipath (σ_m) by:

$$\sigma_m = \frac{\rho \theta_{b1}}{K_m \sqrt{2 G_s}}$$

where

σ_m = rms angle multipath error in same units as θ_{b1}

θ_{b1} = one-way antenna beamwidth

ρ = earth's surface reflectivity

G_s = power ratio of tracking-antenna sum-pattern peak to the error-pattern peak sidelobe at the angle of arrival of the image signal.

Multipath errors, in general, apply only to elevation angle measurements. However, azimuth errors do result from inclined reflecting surfaces and from rough surfaces at any angle. When a smooth, inclined surface reflects energy into the antenna, the multipath error computed for elevation measurement is merely rotated through the angle of inclination, producing a component in azimuth proportional to the size of that angle.

(6) Converter and Quantization Noise

The statements in Paragraph VIa (4) regarding this subject are also true of angle errors. However, it is necessary to distinguish between angle errors and phase quantization errors, which are discussed in the following section.

(7) Quantization Error

Many different types of phase shifters are suitable for steering phased arrays. Primarily, phase shifting or phase shifters are digitally controlled, and therefore, can be set to an accuracy that is a function of the number of bits. The number of bits used affects the gain, sidelobes, and beam pointing accuracy of the array.

The loss in gain of the array (ΔG) is determined by

$$\Delta G = \frac{\pi^2}{(3) 2^{2P}}$$

ΔG is loss in gain

P is number of bits in the phase shifter

The accurate determination of the direction of targets is made by knowing the direction in which the beam pattern or patterns are pointed. With quantized phase shifter, the position of the beam can be moved with a granularity that is a function of the bit size with an absolute accuracy of (assuming symmetric pairs in elements phasing):

$$\Delta\theta = \theta_b \text{ (scanned)} \frac{9}{2^{PN}}$$

where

$\Delta\theta$ is pointing accuracy

N is the number of elements across the aperture

P is the number of phase shifter bits

θ_b (scanned) is the scanned beamwidth, equal to

$$\theta_b \text{ (scanned)} = \frac{\theta_b}{\cos \theta}$$

(8) Mechanical Steering Errors

Mechanically steered antennas suffer from many sources of error. Factors in the design which cause mechanical errors are:

- a) Mechanical deflection of the antenna caused by acceleration.
- b) Electrical noise and drift in servo amplifiers.
- c) Alignment of radar axis with coordinate system.
- d) Precision of the bearings, coupling, and gears.

(9) Boresight Axis

The alignment of the beam with the face of the array is preformed using an anechoic chamber. The alignment error should be adjusted to less than 0.01 mil. If a tower is used for alignment and the tower is located such that surrounding terrain causes multipath errors that are not cancelled out, then the boresight axis error that can be expected is between 0.05 and 0.1 mil rms, corresponding to elevation sidelobe levels of 30 to 35 dB at the off-axis angle equal to twice the tower elevation angle.

(10) Angle Glint

One of the most confused and multi-named terms in the angular error problem is glint, sometimes referred to as angle noise, angle scintillations, angle fluctuation, or target glint. In this discussion, glint is described as angle fluctuations or errors caused by multiple reflectors, much the same as range glint was described. The term "scintillation" will be reserved for amplitude variations that affect angle measurement, whereas glint is due to phase variations. Multiple scatters cause both glint and scintillation.

Because of the complex nature of most targets, discussion of scatter from more than two points is beyond the scope of this technical report.

A simple model of a complex target is two independent isotropic scatterers separated by an angle (θ_B). This target would approximate a fighter aircraft with wing tanks, two aircraft or reentry vehicles in the same radar resolution cell, or a low-flying craft with its ground reflection. The ratio between the radar cross section of the two scatters (σ_R) is assumed to be less than one and the relative phase difference is the angle (α). If the angle error ($\Delta\theta$), is measured from the larger of the two scatterers, then:

$$\frac{\Delta\theta}{\theta_0} = \frac{\sigma_R^2 \sigma_R \cos \alpha}{1 + \sigma_R^2 + 2\sigma_r \cos \alpha}$$

When $\Delta\theta/\theta_0 = 0$, the center is on the larger scatter, and at $\Delta\theta/\theta_0 = 1$, the center is on the smaller scatter.

Although the probability density of glint noise has an infinite standard deviation, the radar output will remain finite because of the restricted dynamic range and bandwidth of the processing circuits. A Gaussian curve may be fitted which will represent the apparent target, thus allowing glint (σ_0) to be expressed as the probability of exceeding the physical limits of the target. Therefore, glint (σ_0) can be expressed as a function of the range (R) and the effective span of the target (L_x) perpendicular to the antenna main beam.

$$\begin{aligned} \sigma_\theta &= 0.35 L_x/R && \text{(radians)} \\ &= 335 L_x/R && \text{(mils)} \end{aligned}$$

where L_x and R are in the same units.

This equation shows quite clearly that if the target is small and range is long, this term can effectively be zero.

(11) Scintillation

As in the discussion of glint, scintillation will be used to describe amplitude fluctuations that effect angle accuracy.

Monopulse angle-measurement systems are not affected by scintillation at high signal-to-noise ratios because the measurement is made on a single pulse rather than on a series of pulses.

The scintillation component of echo power can be considered as noise entering the error detector, and that portion of the scintillation power which is near the scanning frequency (f_s) will produce an error at the output in conical scanning systems. The resulting tracking error caused by scintillation is

$$\sigma_s = \frac{0.27 \theta_b \sqrt{f_g Br}}{f_s}$$

where

θ_b = is the beamwidth of the antenna

f_s = is the scanning frequency

f_g = is the half-power frequency of the scintillation

B_n = is the noise bandwidth of the servo system.

If tracking is maintained by use of a beacon, the modulation on the return signal can have the same effect as scintillation but can be removed by proper design of the beacon.

Both glint and scintillation errors are basically short-range tracking problems and have little affect at long ranges.

c. Velocity Errors

Successive measurements of a range give the rate of change of range with time, or relative velocity. However, the Doppler frequency shift produced by a moving target also provides a measure of relative velocity. When it can be employed, Doppler is usually preferred to successive range measurements because it can achieve a more accurate measurement in a shorter time.

When a target is illuminated by a wave at the operating frequency of the radar (f_0), the received wave will be shifted in frequency by an amount called the Doppler shift, (f_d) according to the Doppler equation:

$$\begin{aligned} f_d &= f_0 \left[\frac{c - v_R}{c + v_r} - 1 \right] \\ &= \frac{2 f_0 v_R}{c} \left[1 - \frac{v_R}{c} + \left(\frac{v_R}{c}\right)^2 - \left(\frac{v_R}{c}\right)^3 + \dots \right] \end{aligned}$$

where

v_R is the time derivative of range (positive for outbound targets).

c is the velocity of light.

The relative contribution of the second-order terms is less than 30 parts per million in (f_d). Therefore,

$$f_d = \frac{-2 f_0 v_r}{c} \quad \text{or} \quad \frac{-2 v_r}{\lambda}$$

The relative velocity of the target is a function of the true velocity as expressed by:

$$v_R = v \cos \theta_t$$

where

θ_t is the angle made by the target trajectory and the line joining the radar and target.

(1) Thermal Noise

The amount of noise in the system relative to the signal level has the same influence on velocity or Doppler measurement that it exerted in Paragraph VIa and VIb.

The rectangular pulse of duration (τ) will have an error component of

$$\sigma_f = \frac{\sqrt{3/2}}{\pi\tau \sqrt{S/n} \sqrt{B\tau}}$$

where

σ_f is rms error in frequency measurement

B is bandwidth

τ is pulse width

S/N is signal-to-noise power ratio

A linear FM pulse compression signal of duration (τ) will have a root-mean-square (rms) frequency error of

$$\sigma_{fc} = \frac{1}{2\tau \sqrt{S/n}}$$

The associated velocity error can be found by the use of either of these equations to determine velocity from frequency shift. The longer the pulse width, the better the accuracy of the frequency measurement.

(2) Multipath Doppler Error

The multipath Doppler error appears as a second signal component related to the direct signal by the reflectivity of the surface (ρ) and the sidelobe attenuation gain of the antenna $\sqrt{G_D/G_R}$.

The rms value of the multipath error in frequency is

$$\sigma_m = \frac{\sqrt{2} h_R \rho \dot{E}}{\lambda \sqrt{GD/GR}}$$

where

- h_R is antenna height above the surface
- ρ is surface reflectivity
- \dot{E} is elevation angle rate
- λ is wavelength

The elevation angle rate is determined from the velocity vector and target range.

$$\dot{E} = \frac{V_t \cos \alpha_t}{R}$$

where

- V_t is target velocity
- α_t is the angle in the vertical plane between the radar beam and the target velocity vector
- R is range to target

The multipath error should be small in a narrow beam system with good sidelobe rejection. As the height of the antenna is increased, the FM sidebands representing the reflected component may fall outside the bandpass of the discriminator.

(3) Oscillator

The ability to hold the radar's transmitter frequency at its intended value is limited by the accuracy and stability of the basic oscillators. Oscillators stability was discussed in Section XIa (3), where it was pointed out that stability on the order of one part in 10^9 can be easily obtained. By combining the short term stability of a crystal oscillator with the accuracy of an atomic standard, the transmitter frequency can be kept with 0.1 Hz of its nominal value.

(4) Voltage Control Oscillator Frequency Lag

A voltage control oscillatory (VCO) ideally matches the target signal shift on a cycle-by-cycle basis. The VCO output is usually multiplied to obtain a higher frequency suitable for direct counting with the required accuracy, or a measurement system must be designed that can interpolate within 1 hertz or the output. Either way, the phase stability of the VCO and its measuring, will be critical. However, because the VCO must follow an accelerating target, the associated lag error can limit the accuracy to the order of 0.1 Hz.

(5) Discrimination Zero Setting

If the crossover point where the filters produce equal outputs is not accurately set to the offset frequency defined by the coherent oscillators, or if it shifts with time, the entire doppler loop will operate with a bias error. Crystal controlled discriminators have an inherent stability on the order of 1 Hz or less in the 100-kHz region. The use of a phase-lock system eliminates this bias component completely.

VII. SUMMARY

Not all signal processing techniques were discussed in this report; only the most prominent were covered. Signal processing techniques are being devised at a rapid rate and each must be analyzed separately.

While the analysis given was for attacking land combat targets, few adjustments are required to modify most of these equations to the air defense role.

DISTRIBUTION

	No. of Copies
Commander White Sands Missile Range ATTN: STEWS-AD-L White Sands Missile Range, NM 88002	1
Sandia Laboratories ATTN: W. H. Curry Div. 1336, Box 5800 Albuquerque, NM 87115	1
Commander US Army Armor Center and Fort Knox ATTN: ATZK-CD-MS Fort Knox, KY 40121	1
Jet Propulsion Laboratory California Institute of Technology ATTN: Library/Acquisitions 111-113 4800 Oak Grove Drive Pasadena, CA 91103	1
Commander (4253-3) Pacific Missile Test Center Point Mugu, CA 93042	1
Sandia Laboratories ATTN: Library P. O. Box 969 Livermore, CA 94550	1
Commandant US Army Air Defense School ATTN: ATSA-CD-MM Fort Bliss, TX 79916	1
Technical Library Naval Ordnance Station Indian Head, MD 20640	1
HQ SAC/NRI (Stinfo Library) Offutt Air Force Base, NE 68113	1
Commander Rock Island Arsenal ATTN: SARRI-RLPL-Technical Library Rock Island, IL 61201	1

	No. of Copies
Commander (Code 233) Naval Weapons Center ATTN: Library Division China Lake, CA 93555	1
DRSMI-LP, Mr. Voigt	1
-R	1
-RPR	15
-REG, Mr. Russell	100
-RPT (Record Copy)	1
(Reference Copy)	1
Director Applied Technology Lab USARTL (AVRADCOM) ATTN: DAVDL-ATL-ASW (J. Shostak) Ft. Eustis, VA 23604	5
Commander US Army ARRADCOM Bldg. 95 North DRDAR-SCF/IM (ATTN: W. Donnally) Dover, N.J. 07801	5
Chief Office of Missile Electronic Warfare US Army Electronic Warfare Lab ERADCOM ATTN: DELEW-M-STE W. Hilbert White Sands Missile Range, N.M. 88002	5
Department of the Army US Army Research Office ATTN: Information Processing Office P. O. Box 12211 Research Triangle Park, NC 27709	1
ADTC (DLOSL) Eglin Air Force Base, FL 32542	1
US Army Command and General Staff College ATTN: ATSW-ET-L Fort Leavenworth, KS 66027	1
University of California Los Alamos Scientific Laboratory ATTN: Reports Library P. O. Box 1663 Los Alamos, NM 87545	1

No. of Copies

Commander USACACDA ATTN: ATCA-CA Fort Leavenworth, KS 66027	1
Library US Army War College Carlisle Barracks, PA 17013	1
IIT Research Institute ATTN: GACIAC 10 West 35th Street Chicago, IL 60616	
Director US Army Ballistic Research Laboratory ATTN: DRDAR-TSB-S (STINFO) Aberdeen Proving Ground, MD 21005	1
US Army Materiel Systems Analysis Activity ATTN: DRXSY-MP Aberdeen Proving Ground, MD 21005	1
US Army Cold Region Research and Engineering Laboratory ATTN: CRREI-RT (Burger) P. O. Box 282 Hanover, NH 03755	1